LETTER

https://doi.org/10.1038/s41586-019-1521-8

Salmonella persisters promote the spread of antibiotic resistance plasmids in the gut

Erik Bakkeren[1], Jana S. Huisman[2,3], Stefan A. Fattinger[1,4], Annika Hausmann[1], Markus Furter[1], Adrian Egli[5,6], Emma Slack[1,7], Mikael E. Sellin[4], Sebastian Bonhoeffer[2], Roland R. Regoes[2], Médéric Diard[1,8,9]* & Wolf-Dietrich Hardt[1,9]*

The emergence of antibiotic-resistant bacteria through mutations or the acquisition of genetic material such as resistance plasmids represents a major public health issue[1,2]. Persisters are subpopulations of bacteria that survive antibiotics by reversibly adapting their physiology[3–10], and can promote the emergence of antibiotic-resistant mutants[11]. We investigated whether persisters can also promote the spread of resistance plasmids. In contrast to mutations, the transfer of resistance plasmids requires the co-occurrence of both a donor and a recipient bacterial strain. For our experiments, we chose the facultative intracellular entero-pathogen *Salmonella enterica* serovar Typhimurium (*S.* Typhimurium) and *Escherichia coli*, a common member of the microbiota[12]. *S.* Typhimurium forms persisters that survive antibiotic therapy in several host tissues. Here we show that tissue-associated *S.* Typhimurium persisters represent long-lived reservoirs of plasmid donors or recipients. The formation of reservoirs of *S.* Typhimurium persisters requires *Salmonella* pathogenicity island (SPI)-1 and/or SPI-2 in gut-associated tissues, or SPI-2 at systemic sites. The re-seeding of these persister bacteria into the gut lumen enables the co-occurrence of donors with gut-resident recipients, and thereby favours plasmid transfer between various strains of Enterobacteriaceae. We observe up to 99% transconjugants within two to three days of re-seeding. Mathematical modelling shows that rare re-seeding events may suffice for a high frequency of conjugation. Vaccination reduces the formation of reservoirs of persisters after oral infection with *S.* Typhimurium, as well as subsequent plasmid transfer. We conclude that—even without selection for plasmid-encoded resistance genes—small reservoirs of pathogen persisters can foster the spread of promiscuous resistance plasmids in the gut.

S. enterica and *E. coli* strains contain numerous resistance plasmids[13,14], and different strains frequently colonize the same host[15–19]. High cell densities in the gut lumen allow high rates of plasmid transfer within and between species[20–22]. *S.* Typhimurium strains can colonize the gut lumen and survive within the tissues of their host for prolonged periods[5–7,15–17,23]. In the absence of suitable resistance genes, the gut-luminal population of *S.* Typhimurium is eliminated by antibiotics within a few hours, whereas tissue-associated *S.* Typhimurium persister cells survive for more than ten days[5–8,24] (Supplementary Discussion). After withdrawal of antibiotics, surviving cells can migrate to the gut lumen and resume growth[24]. We hypothesized that this promotes the co-occurrence of donors with gut-luminal recipients, and thereby fuels the transfer of resistance plasmids in vivo (Extended Data Fig. 1a).

Wild-type *S.* Typhimurium SL1344 naturally carries P2, a well-characterized conjugative plasmid of the IncI1 incompatibility group[25] in Enterobacteriaceae[20–22] (Extended Data Fig. 1b); this strain of *S.* Typhimurium served as the donor in our initial experiments. We labelled P2 with a chloramphenicol-resistance marker ($P2^{cat}$) to monitor plasmid transfer by plating (Extended Data Fig. 1c, d). Controls excluded cross-resistance for any of the resistance markers used in this study (Extended Data Fig. 2). In the 'oral model', the donor (that is, *S.* Typhimurium $P2^{cat}$) initially colonized the gut lumen and invaded host tissues (Fig. 1a, b, Extended Data Fig. 3). Ciprofloxacin cleared the gut-luminal bacteria, whereas tissue-associated *S.* Typhimurium $P2^{cat}$ persisters survived[5–8]. The recipient *S.* Typhimurium ATCC 14028S strain, which naturally lacks P2, was introduced at day 8[21,22]. Transconjugants (that is, recipients that obtained the plasmid) replaced the recipients within one to three days of donor re-seeding (>99% median; day 11–12 of the experiment) (Fig. 1c, Extended Data Fig. 3a). Control experiments refuted that the replacement by transconjugants is attributable to P2-mediated fitness benefits over the recipients (Extended Data Fig. 3d, e). Further control experiments verified that $P2^{cat}$ transfer occurs in the gut lumen (Extended Data Fig. 3f, g) and that $P2^{cat}$ spreads by conjugation (Extended Data Fig. 3h, i). Non-invasive donor mutants indicated that the donor cells originated from reservoirs of tissue-associated *S.* Typhimurium $P2^{cat}$ persisters (Fig. 1c–e, Extended Data Figs. 3b, 4). However, this cannot definitively rule out that rare persisters could also exist in the gut lumen.

To verify the importance of reservoirs of tissue-associated *S.* Typhimurium persisters, we used an 'intravenous infection model' (Fig. 2a, b). Consistent with previous work[23], *S.* Typhimurium $P2^{cat}$ formed large populations of persisters that survived in the spleen and the liver after intraperitoneal treatment with ceftriaxone (Fig. 2c, d, Extended Data Fig. 5a). In contrast to the oral model, gut-luminal colonization by *S.* Typhimurium $P2^{cat}$ is observed only very rarely by day 5 (Extended Data Fig. 5). Nevertheless, when donors were detected in the gut lumen, transconjugants were formed with high efficiency within one to three days (Fig. 2e, Extended Data Fig. 5b). Donors that lacked a key virulence factor that promotes both systemic growth of pathogens in vivo[26] and the survival of persisters[27] yielded much smaller reservoirs of persisters than did wild-type *S.* Typhimurium $P2^{cat}$ (Fig. 2d), and did not produce transconjugants (Fig. 2e, Extended Data Fig. 5c). We conclude that tissue-associated *S.* Typhimurium persisters can serve as reservoirs that promote the spread of conjugative plasmids.

We next identified the rate-limiting process in transconjugant formation in vivo, focusing on the oral model. Three key parameters may dictate plasmid transfer dynamics: (1) the rate at which plasmid-carrying donors re-enter the gut lumen and perform the initial conjugation event (that is, re-seeding), which is dependent on the size of the reservoir of persisters; (2) the rate of plasmid transfer from transconjugants to recipients; and (3) the relative growth rate of transconjugants compared to recipients. To estimate these rates, we used donor mixtures that carried five variants of DNA-tagged $P2^{cat}$ (*S.* Typhimurium $P2^{cat\,tag}$) (Extended Data Fig. 6). Whereas all tags were present in roughly equivalent abundance in the inoculum, the faeces (on day 1) and the mucosa (on day 15), most transconjugant populations contained just

[1]Institute of Microbiology, Department of Biology, ETH Zurich, Zurich, Switzerland. [2]Institute of Integrative Biology, Department of Environmental Systems Science, ETH Zurich, Zurich, Switzerland. [3]Swiss Institute of Bioinformatics, Lausanne, Switzerland. [4]Science for Life Laboratory, Department of Medical Biochemistry and Microbiology, Uppsala University, Uppsala, Sweden. [5]Division of Clinical Microbiology, University Hospital Basel, Basel, Switzerland. [6]Applied Microbiology Research, Department of Biomedicine, University of Basel, Basel, Switzerland. [7]Institute of Food, Nutrition and Health, Department of Health Sciences and Technology, ETH Zurich, Zurich, Switzerland. [8]Biozentrum, University of Basel, Basel, Switzerland. [9]These authors contributed equally: Médéric Diard, Wolf-Dietrich Hardt. *e-mail: mederic.diard@unibas.ch; hardt@micro.biol.ethz.ch

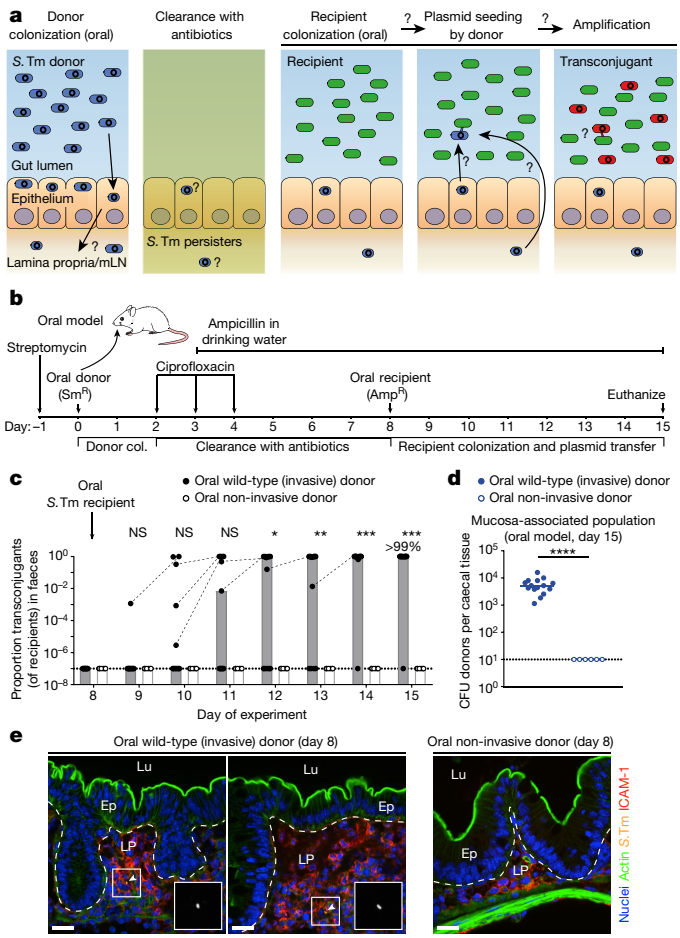

Fig. 1 | *S.* Typhimurium persisters associated with gut tissue are a reservoir for conjugative plasmids. a, Plasmid-bearing *S.* Typhimurium (*S.* Tm) (blue lozenge) form persisters (shown as smaller lozenges) in gut tissues and the mesenteric lymph nodes (mLN). These can survive antibiotic treatment, re-seed the gut lumen and transfer their plasmid to recipients (green). Transconjugants (red) can further amplify the spread of plasmids. **b**, Oral infection mouse model. Col., colonization. **c**, Donor mucosa invasion is required for persister-promoted plasmid transfer. Invasive (streptomycin-resistant (Sm^R) and Cm^R) or non-invasive *S.* Typhimurium SL1344 $P2^{cat}$ strain (TTSS-1-negative, Sm^R and Cm^R) was used as a donor, and *S.* Typhimurium 14028S *aphT* (free of P2) (Kan^R and Amp^R) was used as a recipient, as shown in **b**. Transconjugant proportions in faeces from experiments with invasive (solid black circles; grey bars indicate median; $n = 15$ mice; 5 independent experiments; $n = 9$ mice pooled from data in Fig. 3) or non-invasive donors (open black circles; white bars indicate median; $n = 6$ mice, 2 independent experiments). Dashed lines connect data points from the same mice. **d**, Donor reservoirs in the caecal mucosa from mice, as infected in **c**, were quantified by tissue gentamicin protection. Solid blue circles represent invasive donors; open blue circles represent non-invasive donors; lines indicate the median. Statistics were performed using a two-tailed Mann–Whitney *U*-test. NS, not significant ($P \geq 0.05$), $^*P < 0.05$, $^{**}P < 0.01$, $^{***}P < 0.001$, $^{****}P < 0.0001$. Dotted line denotes the detection limit. **e**, Persisters in the caecum lamina propria (LP) (oral model, day 8). *S.* Typhimurium (yellow, anti-LPS O5 and anti-LPS O12 staining), nuclei (blue), actin (green) and lamina propria (red, ICAM-1) are stained. Ep, epithelium; lu, lumen. Scale bars, 20 μm. White arrows highlight *S.* Typhimurium (magnified in inset). Representative of three independent experiments. Quantification is provided in Extended Data Fig. 4.

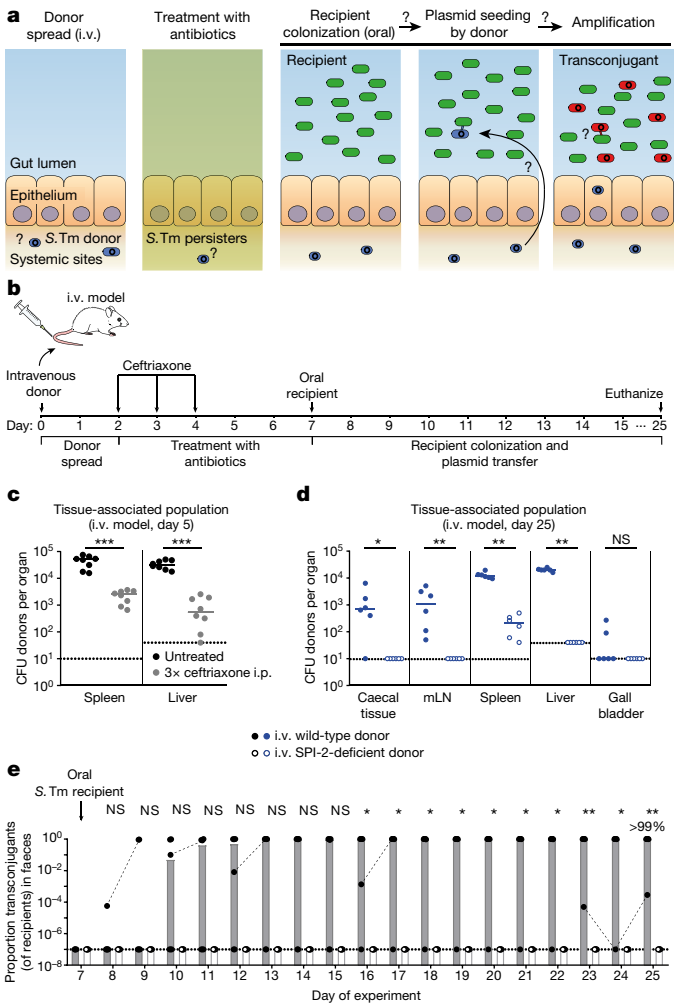

Fig. 2 | Persisters at systemic sites are a reservoir for plasmid transfer in the gut. a, As in Fig. 1a, but donors are introduced by intravenous infection. **b**, Intravenous (i.v.) infection mouse model. **c**, Persisters in the spleens and livers. In two independent experiments, $n = 8$ mice (grey circles) were infected intravenously with an equal mix of five *S.* Typhimurium $P2^{cat\ tag}$ strains (SL1344 strain; Sm^R and Cm^R). Black circles indicate control mice ($n = 8$) infected for 5 days without ceftriaxone treatment. Extended Data Figure 5a shows counts for additional organs. **d**, **e**, SPI-2 promotes donor reservoir formation at systemic sites. In two independent experiments, mice were infected as described in **b** with donors; that is, with mixtures of five wild-type ($n = 6$; closed circles) or SPI-2-deficient ($n = 6$; open circles) *S.* Typhimurium $P2^{cat\ tag}$ strains (Sm^R and Cm^R). **d**, Donor populations in internal organs from mice infected with wild-type (solid blue) or SPI-2-deficient donors (open blue). Lines indicate the median. **e**, Faecal populations from mice from **d**. Proportions of transconjugants in faeces, from experiments with wild-type (solid black circles; grey bars indicate median) or non-invasive donors (open black circles; white bars indicate median). Dashed lines connect data points from the same mice. Statistics were performed using a two-tailed Mann–Whitney *U*-test. NS, not significant ($P > 0.05$), $^*P < 0.05$, $^{**}P < 0.01$, $^{***}P < 0.001$. Dotted lines denote detection limits.

one or two of the five tags (Fig. 3a, b, Extended Data Fig. 6b, c). In the intravenous-infection experimental setup (Fig. 2b, e), transconjugants were also dominated by only one tag (Extended Data Fig. 6d–f). Transconjugant populations therefore arise from very few donor-to-recipient conjugation events, followed by transconjugant-to-recipient spread.

To quantify the relative contribution of donor re-seeding and plasmid conjugation, we developed a mathematical model (Extended Data Fig. 6g). This model assessed the interdependence of the rate of donor re-seeding (η, the sum of donor re-seeding plus the donor-to-recipient conjugation) and the rate of transconjugant-to-recipient conjugation (γ) (Supplementary Information). Fitting our mathematical model to the distributions of the plasmid tags confirmed that η is rate-limiting, and identified the most-likely parameters; these were per-recipient rates of $\eta = 3.16 \times 10^{-10}$ re-seeding events per day and $\gamma = 3.16 \times 10^{-8}$ conjugation events per colony-forming unit (CFU) per gram of

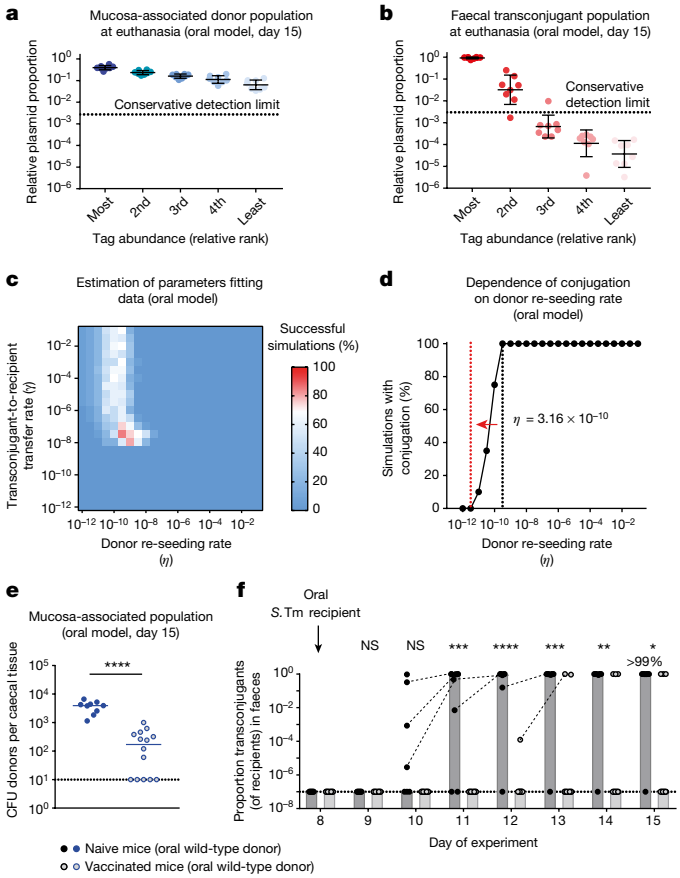

Fig. 3 | Plasmid transfer is initiated by rare re-seeding events from donors and can be prevented by vaccination. Mice were orally infected (Fig. 1b) with tagged donor (five *S.* Typhimurium P2$^{cat\ tag}$ SL1344 strains; Sm^R and Cm^R) and recipient mixtures (five tagged *S.* Typhimurium 14028S strains; Kan^R and Amp^R). $n = 8$ mice, 3 independent experiments. Donors, recipients and transconjugants were enumerated by plating (Extended Data Fig. 7a) and plasmid-tag distributions were analysed by quantitative PCR (qPCR) (raw data shown in Extended Data Fig. 6b). **a**, **b**, Plasmid-tag distribution in mucosa-associated donors and faecal transconjugants at day 15. Dotted lines indicate conservative qPCR detection limits (2.9×10^{-3}). Line indicates mean; error bars indicate s.d. **c**, Modelling results. Simulations are described in the Supplementary Information. A rate of donor re-seeding and donor-to-recipient conjugation of $\eta = 3.16 \times 10^{-10}$ events per recipient per day, and a rate of transconjugant-to-recipient conjugation of $\gamma = 3.16 \times 10^{-8}$ events per recipient per CFU per gram of faeces per day, optimally fit the data (red). **d**, Effect of η on transconjugant detection. Analysis as described in the Supplementary Information. Reducing η by 100-fold below the value estimated for naive mice (black dotted line; $\eta = 3.16 \times 10^{-10}$ events) diminishes transconjugant detection (red dotted line). **e**, **f**, Vaccination diminishes conjugation. Mice vaccinated with killed *S.* Typhimurium (open circles; $n = 14$ mice, 4 independent experiments) or PBS (naive; closed circles; $n = 9$ mice, 3 independent experiments) were infected with tagged donor and recipient mixtures as in **a** and **b**. Donors, recipients and transconjugants were enumerated by plating. **e**, Mucosa-associated donor populations at day 15. **f**, Faecal transconjugant proportions in naive (black circles; grey bars indicate median) or vaccinated mice (light grey circles; light grey bars indicate median) from **e**. Dashed lines connect data points from the same mice. Statistics were performed using a two-tailed Mann–Whitney *U*-test. NS, not significant ($P \geq 0.05$), *$P < 0.05$, **$P < 0.01$, ***$P < 0.001$, ****$P < 0.0001$. Dotted lines denote detection limits.

faeces per day (red in Fig. 3c; marginal posterior densities are listed in Supplementary Table 4). This corresponds to approximately 1.6 donor re-seeding events (plus the initial plasmid transfer) per day into the gut lumen. By contrast, transconjugant-to-recipient plasmid conjugation rates were ≥32 events per day for the initial conjugations, and increased exponentially thereafter (Supplementary Information).

We then used our mathematical model to predict the effect of reducing the rate of donor re-seeding. The transconjugant-to-recipient conjugation parameter was fixed at $\gamma = 3.16 \times 10^{-8}$ events per CFU per gram of faeces per day (Fig. 3c), and we evaluated the probability of conjugation events occurring within the course of our 15-day experiment (Fig. 3d). Reducing η by more than 100-fold diminished conjugation (Fig. 3d). To test this prediction, we used oral vaccination with killed *S.* Typhimurium cells[28], a procedure that is known to reduce *S.* Typhimurium invasion of the gut tissue. Consistent with previous work[22], vaccinated mice contained 10–500-fold smaller reservoirs of persisters than did naive mice (Fig. 3e). Indeed, this vaccination prevented plasmid transfer in the vast majority of mice (Fig. 3f, Extended Data Fig. 7a–c). Moreover, the transconjugants detected in vaccinated mice appeared later than the transconjugants in non-vaccinated controls (Fig. 3f). Control experiments with reduced fractions of invasive donors verified this observation (Extended Data Fig. 7d–g). Thus, the size of the tissue-associated reservoir of persisters is a main driver of the ensuing rise of transconjugants. These data confirm the predictions of our mathematical model (Fig. 3d) and suggest that vaccination might provide a means to prevent the formation of mucosa-associated reservoirs of conjugative plasmids.

We next addressed whether strains of the microbiota could also acquire these conjugative plasmids. First, we analysed P2^{cat} transfer to the commensal *E. coli* strain 8178[20,22]. For this purpose, we created an ampicillin-resistant derivative of *E. coli* 8178 that was free of the P2 plasmid[20], and used it as a recipient in the oral model (Fig. 1b). This yielded efficient plasmid transfer (Fig. 4a, b, Extended Data Fig. 8a). We tested whether tissue-associated *S.* Typhimurium persisters could also serve as recipients. In the oral model (Fig. 1b), mice were first infected with a P2-cured variant of *S.* Typhimurium SL1344 (kanamycin-resistant (Kan^R)). Then, we treated the mice with ciprofloxacin and ampicillin, and introduced the donor (*E. coli* 8178 P2^{cat}; ampicillin-resistant (Amp^R) and chloramphenicol-resistant (Cm^R)). *S.* Typhimurium re-seeded the gut lumen and transconjugants were formed (>38% median) (Extended Data Fig. 8b–d). Thus, tissue-associated *S.* Typhimurium persisters can serve as donors or as recipients of plasmid transfer between different species of Enterobacteriaceae.

To assess whether mucosa-associated *S.* Typhimurium can also serve as a reservoir for clinically relevant plasmids that carry genes of the extended-spectrum β-lactamase (ESBL) family, we used pESBL15 (Extended Data Fig. 1b). *S.* Typhimurium SL1344 pESBL15 was used as a donor. We modified our oral model from Fig. 1b in two ways: by replacing ampicillin with kanamycin in the drinking water, and by using an ampicillin-sensitive (Amp^S), but Kan^R, variant of our standard recipient strain (*S.* Typhimurium 14028S *aphT* (Kan^R and Amp^S)). We observed tissue-associated persisters, re-seeding of the gut lumen and efficient plasmid transfer (Fig. 4c, d, Extended Data Fig. 8e). Thus, our findings apply to clinically important resistance plasmids. The choice of the antibiotics used for the different phases of our oral model had little effect on these fast plasmid-transfer kinetics (Extended Data Fig. 9a–d).

Finally, we validated the transfer of antibiotic-resistance plasmids to *E. coli* in the intravenous model. Intravenous infection of *S.* Typhimurium P2^{cat} led to populations of persisters in the internal organs (Fig. 4e); these populations could re-seed the gut lumen and transferred the plasmid into the luminal recipient population, forming >25% *E. coli* transconjugants in the absence of antibiotic selection (Fig. 4f, Extended Data Fig. 9e). Thus, tissue-associated *S.* Typhimurium persisters can serve as a reservoir for resistance plasmids that can be efficiently transferred to different species of Enterobacteriaceae.

Our results uncover a mechanism by which antibiotic persistence promotes the spread of antibiotic-resistance plasmids, specifically by promoting the co-occurrence of donors and recipient bacteria in the gut-luminal niche. This reveals a role for persistence in clinical bacterial infection: not only can bacterial persistence lead to relapse of disease in chronic infections, but also it can facilitate the spread of antibiotic resistance. In the case discussed here, the transfer rate is independent

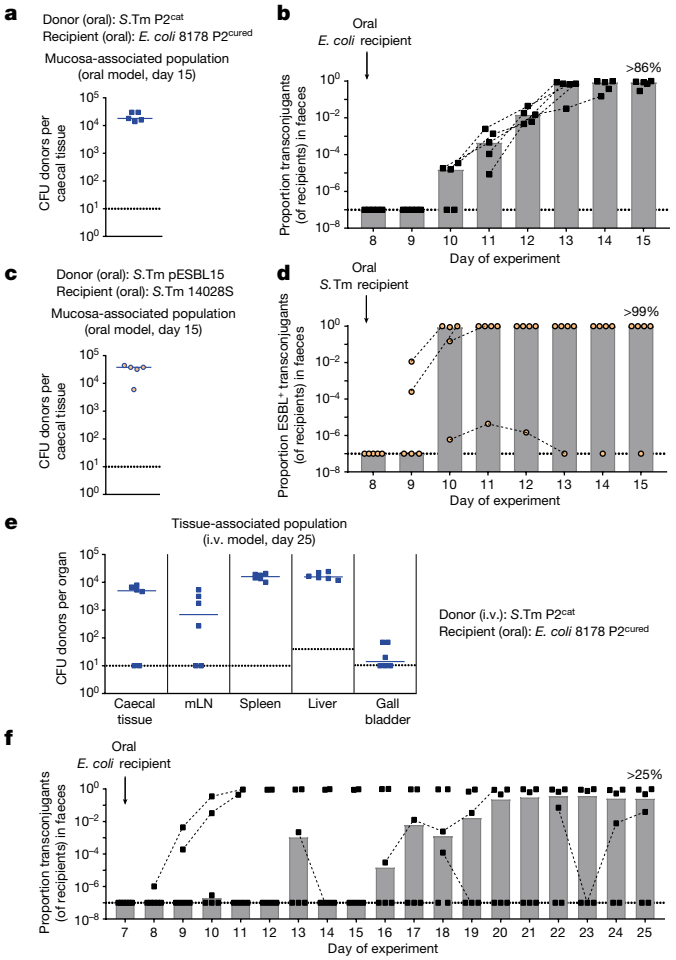

Fig. 4 | Tissue-associated persisters promote the transfer of resistance plasmids between different species of Enterobacteriaceae. a, **b**, Plasmid transfer to *E. coli*. Five mice (one experiment) were infected orally as described in Fig. 1b (except that ampicillin was removed from the drinking water on day 8), with donors (*S.* Typhimurium P2^{cat} SL1344 strain, Sm^{R} and Cm^{R}) and recipients (*E. coli* 8178 P2^{cured} strain, Amp^{R}). Mucosa-associated donors and faecal transconjugants were enumerated by plating. Median indicated by solid line or bars. **c, d**, Transfer of plasmids containing ESBL genes between *Salmonella* spp. The experiment used *S.* Typhimurium SL1344 pESBL15 (Sm^{R} and Amp^{R}) as the donor and *S.* Typhimurium 14028S *aphT* (Kan^{R}) as the recipient ($n = 5$ mice, 1 experiment). This experiment was performed and evaluated as in **a**, **b**, except that kanamycin was used in the drinking water from day 3 to day 8 (instead of ampicillin, as pESBL15 confers ampicillin resistance). **e, f**, Plasmid transfer from *S.* Typhimurium to *E. coli* using the intravenous model. Six mice (two independent experiments) were infected as described in Fig. 2b, with donors (*S.* Typhimurium P2^{cat} SL1344 strain (Sm^{R} and Cm^{R}), intravenous) and recipients (*E. coli* 8178 P2^{cured} (Amp^{R}), oral). Tissue-associated donors and faecal transconjugants were enumerated by plating. Median indicated by solid line or bars. **a**–**f**, Dotted lines indicate detection limit by selective plating. **b**, **d**, **f**, Dashed lines connect data points from the same mice to illustrate the progression of plasmid spread after initial detection.

of selective pressures for the functions encoded on the plasmid. Thus, in the absence of antibiotic-driven selection, resistance genes on promiscuous plasmids can spread from a very small number of donor cells that co-occur with dense recipient-cell populations.

Mathematical modelling showed that re-seeding is the rate-limiting aspect of this process, and suggested that reducing the tissue-associated population of *S.* Typhimurium (for example, through vaccination) could reduce plasmid re-seeding to negligible levels. As re-seeding events are rare compared to the number of tissue-associated persisters, such persister-promoted spread of plasmids may last for weeks or months after an acute infection. We do not yet know whether this translates to infections in livestock or humans, during which tissue-associated reservoirs of persisters might be smaller.

Associations between persistence and chronic infections occur in a variety of clinical contexts[29] and in biofilms[30]. Therefore, reservoirs for conjugative plasmids could exist in a multitude of populations of persisters. In the two mouse models discussed here, *S.* Typhimurium persisters associated with different organs appear to be capable of re-seeding the gut lumen. The intracellular environment in classical dendritic cells[7] or macrophages[6] can induce persistence. In contrast to infected epithelial cells[31,32], these phagocytes are long-lived, which suggests that they hold most of the donor persisters in both the oral and the intravenous model. The difference between the location of the reservoir of persister cells in the oral (lamina propria and mesenteric lymph nodes) and the intravenous (spleen, liver and gall bladder) models, and the differential requirement for SPI-1- and SPI-2-encoded virulence factors, indicate that there are diverse mechanisms through which tissue-associated *S.* Typhimurium persisters can establish a reservoir, survive and—ultimately—re-seed the gut lumen to engage in plasmid transfer.

The link between persistence and plasmid-mediated evolution of antibiotic resistance may be particularly relevant in the farming industry, in which *S. enterica* has a high prevalence and animals are often co-colonized by strains of *Salmonella* and *E. coli*. There can be two *Salmonella* strains within the same host, one within lymphoid tissues (for example, mesenteric lymph nodes) and the other in the intestinal content[17]. This is also consistent with the isolation of *Salmonella* spp. from intestinal biopsies in swine that have chronic subclinical *Salmonella* infections, indicating that reservoirs of pathogen persisters are common in the gut mucosa of these animals[15,16]. Our results suggest that this may promote the spread of resistance plasmids in animal herds.

Strategies to reduce bacterial persistence are of general importance[33]. This is relevant not only for the clinical treatment of infected individuals[29], but also to minimize the effect of persistence on the global evolution of antibiotic resistance via both resistance mutations[11] and resistance plasmid spread, as shown here. Inactivated vaccines, such as the *Salmonella* cells killed by peracetic acid that we use here, should be easily and safely applicable[28]. Our data show that vaccination efficiently prevents tissue invasion and disease, and minimizes the size of persister reservoirs—and thereby reduces the subsequent spread of resistance plasmids, such as those encoding ESBL proteins (Fig. 3).

Online content

Any methods, additional references, Nature Research reporting summaries, source data, extended data, supplementary information, acknowledgements, peer review information; details of author contributions and competing interests; and statements of data and code availability are available at https://doi.org/10.1038/s41586-019-1521-8.

Received: 18 October 2018; Accepted: 5 August 2019;
Published online 4 September 2019.

1. Parisi, A. et al. Health outcomes from multidrug-resistant *Salmonella* infections in high-income countries: a systematic review and meta-analysis. *Foodborne Pathog. Dis.* **15**, 428–436 (2018).
2. Wright, G. D. The antibiotic resistome: the nexus of chemical and genetic diversity. *Nat. Rev. Microbiol.* **5**, 175–186 (2007).
3. Brauner, A., Fridman, O., Gefen, O. & Balaban, N. Q. Distinguishing between resistance, tolerance and persistence to antibiotic treatment. *Nat. Rev. Microbiol.* **14**, 320–330 (2016).
4. Fridman, O., Goldberg, A., Ronin, I., Shoresh, N. & Balaban, N. Q. Optimization of lag time underlies antibiotic tolerance in evolved bacterial populations. *Nature* **513**, 418–421 (2014).
5. Claudi, B. et al. Phenotypic variation of *Salmonella* in host tissues delays eradication by antimicrobial chemotherapy. *Cell* **158**, 722–733 (2014).
6. Helaine, S. et al. Internalization of *Salmonella* by macrophages induces formation of nonreplicating persisters. *Science* **343**, 204–208 (2014).
7. Kaiser, P. et al. Cecum lymph node dendritic cells harbor slow-growing bacteria phenotypically tolerant to antibiotic treatment. *PLoS Biol.* **12**, e1001793 (2014).
8. Dolowschiak, T. et al. IFN-γ hinders recovery from mucosal inflammation during antibiotic therapy for *Salmonella* gut infection. *Cell Host Microbe* **20**, 238–249 (2016).

9. Balaban, N. Q. et al. Definitions and guidelines for research on antibiotic persistence. *Nat. Rev. Microbiol*. **17**, 441–448 (2019).
10. Balaban, N. Q., Merrin, J., Chait, R., Kowalik, L. & Leibler, S. Bacterial persistence as a phenotypic switch. *Science* **305**, 1622–1625 (2004).
11. Levin-Reisman, I. et al. Antibiotic tolerance facilitates the evolution of resistance. *Science* **355**, 826–830 (2017).
12. Wotzka, S. Y. et al. Microbiota stability in healthy individuals after single-dose lactulose challenge–a randomized controlled study. *PLoS ONE* **13**, e0206214 (2018).
13. Coque, T. M., Baquero, F. & Canton, R. Increasing prevalence of ESBL-producing Enterobacteriaceae in Europe. *Eurosurveillance* **13**, 19044 (2008).
14. Crump, J. A., Sjölund-Karlsson, M., Gordon, M. A. & Parry, C. M. Epidemiology, clinical presentation, laboratory diagnosis, antimicrobial resistance, and antimicrobial management of invasive *Salmonella* infections. *Clin. Microbiol. Rev*. **28**, 901–937 (2015).
15. Wilcock, B. P., Armstrong, C. H. & Olander, H. J. The significance of the serotype in the clinical and pathological features of naturally occurring porcine salmonellosis. *Can. J. Comp. Med*. **40**, 80–88 (1976).
16. Wood, R. L., Pospischil, A. & Rose, R. Distribution of persistent *Salmonella typhimurium* infection in internal organs of swine. *Am. J. Vet. Res*. **50**, 1015–1021 (1989).
17. San Román, B. et al. Relationship between Salmonella infection, shedding and serology in fattening pigs in low–moderate prevalence areas. *Zoonoses Public Health* **65**, 481–489 (2018).
18. Tenaillon, O., Skurnik, D., Picard, B. & Denamur, E. The population genetics of commensal *Escherichia coli*. *Nat. Rev. Microbiol*. **8**, 207–217 (2010).
19. Apperloo-Renkema, H. Z., Van der Waaij, B. D. & Van der Waaij, D. Determination of colonization resistance of the digestive tract by biotyping of Enterobacteriaceae. *Epidemiol. Infect*. **105**, 355–361 (1990).
20. Stecher, B. et al. Gut inflammation can boost horizontal gene transfer between pathogenic and commensal Enterobacteriaceae. *Proc. Natl Acad. Sci. USA* **109**, 1269–1274 (2012).
21. Diard, M. et al. Inflammation boosts bacteriophage transfer between *Salmonella* spp. *Science* **355**, 1211–1215 (2017).
22. Moor, K. et al. High-avidity IgA protects the intestine by enchaining growing bacteria. *Nature* **544**, 498–502 (2017).
23. Monack, D. M., Bouley, D. M. & Falkow, S. *Salmonella typhimurium* persists within macrophages in the mesenteric lymph nodes of chronically infected *Nramp1*$^{+/+}$ mice and can be reactivated by IFNγ neutralization. *J. Exp. Med*. **199**, 231–241 (2004).
24. Diard, M. et al. Antibiotic treatment selects for cooperative virulence of *Salmonella* Typhimurium. *Curr. Biol*. **24**, 2000–2005 (2014).
25. Sampei, G. et al. Complete genome sequence of the incompatibility group I1 plasmid R64. *Plasmid* **64**, 92–103 (2010).
26. Hensel, M. et al. Simultaneous identification of bacterial virulence genes by negative selection. *Science* **269**, 400–403 (1995).
27. Stapels, D. A. C. et al. *Salmonella* persisters undermine host immune defenses during antibiotic treatment. *Science* **362**, 1156–1160 (2018).
28. Moor, K. et al. Peracetic acid treatment generates potent inactivated oral vaccines from a broad range of culturable bacterial species. *Front. Immunol*. **7**, 34 (2016).
29. Fauvart, M., De Groote, V. N. & Michiels, J. Role of persister cells in chronic infections: clinical relevance and perspectives on anti-persister therapies. *J. Med. Microbiol*. **60**, 699–709 (2011).
30. Roberts, M. E. & Stewart, P. S. Modelling protection from antimicrobial agents in biofilms through the formation of persister cells. *Microbiology* **151**, 75–80 (2005).
31. Knodler, L. A. et al. Noncanonical inflammasome activation of caspase-4/caspase-11 mediates epithelial defenses against enteric bacterial pathogens. *Cell Host Microbe* **16**, 249–256 (2014).
32. Sellin, M. E. et al. Epithelium-intrinsic NAIP/NLRC4 inflammasome drives infected enterocyte expulsion to restrict *Salmonella* replication in the intestinal mucosa. *Cell Host Microbe* **16**, 237–248 (2014).
33. Defraine, V., Fauvart, M. & Michiels, J. Fighting bacterial persistence: current and emerging anti-persister strategies and therapeutics. *Drug Resist. Updat*. **38**, 12–26 (2018).

METHODS

No statistical methods were used to predetermine sample size. The experiments were not randomized and investigators were not blinded to allocation during experiments and outcome assessment. This was necessary to avoid cross-contamination of pathogens and plasmid donors between the different experimental groups as far as possible.

Strains and plasmids used in this study. Supplementary Table 1 contains all strains and plasmids used in this study. For cultivation of bacteria, lysogeny broth (LB) medium containing the appropriate antibiotics (50 μg/ml streptomycin (AppliChem), 6 μg/ml chloramphenicol (AppliChem), 50 μg/ml kanamycin (AppliChem) or 100 μg/ml ampicillin (AppliChem)) were used. To create $P2^{cat\ tag}$ strains (using previously published neutral genetic barcodes[34]) or gene-deletion mutants (for example, *oriT*::*aphT* on P2), the λ red system was used, as previously described[35]. If desired, antibiotic-resistance cassettes were removed using the temperature-inducible FLP recombinase encoded on pCP20[35]. Mutations or sequence tags coupled to antibiotic-resistance cassettes were transferred into the desired genetic background using transduction with P22 HT105/1 *int-201*[36]. Primers used for strain construction or verification of genetic background are listed in Supplementary Table 2.

In vitro plasmid-transfer kinetics. Overnight cultures with appropriate antibiotics of donor (SL1344 $P2^{cat}$) and recipient (14028S *aphT*) strains carrying pM975 to confer ampicillin resistance were subcultured 1:20 in LB without antibiotics, and grown for 4 h. Approximately 10^2 CFU of each were added (sequentially as 25-μl volumes) to 450 μl LB with 100 μg/ml ampicillin. Samples were incubated at 37 °C mixing at 1,000 r.p.m. for 24 h. Aliquots (10 μl) were taken every hour, diluted, and plated on selective MacConkey agar for enumeration.

In vitro antibiotic-resistance profiling. Flat-bottom transparent 96-well plates were filled with 100 μl of LB containing twofold dilutions of the specified antibiotic (streptomycin (AppliChem), chloramphenicol (AppliChem), kanamycin (AppliChem), ampicillin (AppliChem), ciprofloxacin (ciprofloxacin hydrochloride monohydrate, Sigma-Aldrich), gentamicin (AppliChem) or ceftriaxone (ceftriaxone disodium salt hemi(heptahydrate), Sigma-Aldrich). Each plate contained eleven twofold dilution steps of each antibiotic, plus a no antibiotic control and a no-bacteria sterility control. Overnight cultures of each bacterial strain tested were grown in the presence of appropriate antibiotics, subcultured (1:20 dilution) for 4 h at 37 °C in LB without antibiotics, and diluted in PBS. Cells were seeded in each well at a final density of 10^5 CFU/ml. Ninety-six-well plates were incubated at 37 °C at 120 r.p.m. for 16 h and the optical density at 600 nm ($OD_{600\ nm}$) was measured. The no-bacteria sterility control was used for background subtraction.

Infection experiments. *Oral infection model.* For in vivo plasmid-transfer experiments, 8–12-week-old 129/SvEv mice were used. These mice are $Nramp1^{+/+}$ (*Nramp1* is also known as *Slc11a1*) and therefore allow for long-term *S.* Typhimurium infections[37]. They carry a complex specified-pathogen-free microbiota without *E. coli*. The experiment has three phases: (1) donor colonization; (2) clearance with antibiotics; and (3) recipient colonization and conjugative transfer. In phase (1), mice were pre-treated with 25 mg streptomycin orally to allow for robust colonization of *S.* Typhimurium[38]. Donor (that is, plasmid-bearing) *S.* Typhimurium was cultivated overnight at 37 °C in LB containing the appropriate antibiotics, subcultured (1:20 dilution) for 4 h at 37 °C in LB without antibiotics, washed with sterile PBS, and 5×10^7 CFU were introduced into mice via oral gavage[38]. In phase (2), 2 days after infection, 3 mg of ciprofloxacin (ciprofloxacin hydrochloride monohydrate, Sigma-Aldrich) dissolved in 100 μl sterile dH_2O was administered by oral gavage for 3 consecutive days. Mice were transferred to fresh cages after each ciprofloxacin treatment to minimize gut recolonization from the environment. Ampicillin (2 g/l) or kanamycin (1 g/l) was added to the drinking water starting at day 3 after infection, and maintained until either day 8 or day 15. This prevented premature donor re-seeding after the cessation of ciprofloxacin treatment. In phase (3), mice were kept individually after ciprofloxacin treatment to prevent cross-contamination owing to coprophagy. Recipient bacteria (that is, plasmid-free *S.* Typhimurium or *E. coli*; 5×10^7 CFU) were orally introduced into mice on day 8 after infection (culture and subculture conditions as above) and populations were monitored for 7 days until they were euthanized (day 15).

Intravenous infection model. The in vivo plasmid-transfer experiment had three phases: (1) donor colonization; (2) clearance with antibiotics; and (3) recipient colonization and conjugative transfer. In phase (1), the donor strain was injected intravenously into the tail vein of 8–12-week-old 129/SvEv mice (10^3 CFU). In phase (2), 2 days after intravenous infection of donors, 1.5 mg of ceftriaxone (ceftriaxone disodium salt hemi(heptahydrate) dissolved in 100 μl PBS, Sigma-Aldrich) was intraperitoneally injected for 3 consecutive days. After the third treatment, mice were transferred to fresh cages and kept individually to prevent cross-contamination owing to coprophagy. In phase (3), the recipient was introduced on day 7 after donor infection (10^8 CFU by gavage) and faecal populations were monitored for 18 days until the mice were euthanized (day 25).

In both infection models, faeces were collected daily, homogenized in PBS with a steel ball at 25 Hz for 1 min and diluted; selective plating on MacConkey agar (supplemented with the appropriate antibiotics) was used to enumerate populations of donors, recipients or transconjugants. The proportion of transconjugants was calculated by dividing the transconjugant population (Cm^R and Kan^R) by the sum of transconjugants and plasmid-free recipients (Kan^R). Lipocalin-2 enzyme-linked immunosorbent assay (ELISA) (R&D Systems kit; protocol according to manufacturer) was performed on faeces to determine the inflammatory state of the gut. When the mice were euthanized (at day 5, 8, 15 or 25, as specified in figure legends), the mesenteric lymph nodes, spleen, liver and gall bladder were collected, homogenized in PBT at 25 Hz for 2 min, and bacteria were enumerated by selective plating. The caecum was removed, opened longitudinally, washed 3 times in PBS, and then placed in 400 μg/ml gentamicin (AppliChem) for 30 min at room temperature. Nine consecutive washing steps in PBS (45 s each) ensured the removal of gentamicin; caecal tissue was subsequently homogenized and mucosa-associated bacteria were enumerated as for the other organs (gentamicin protection modified from a previously published protocol[24]). In Extended Data Fig. 5a, additional organs were collected as indicated in the figure legend. All organs were processed as indicated above. For the jejunum, ileum and colon, 1 cm of intestine was collected, washed briefly in PBS and the tissue (including the majority of the content) was analysed. For analysis of bacteria in the blood, 100 μl of blood was aspirated from the heart immediately after euthanasia and mixed in PBS containing 2% BSA and 1 mM EDTA to prevent coagulation.

For competition experiments, 8–12-week-old 129/SvEv mice were pre-treated with 20 mg ampicillin orally, and ampicillin (2 g/l) was maintained in the drinking water throughout the experiment. The two competitor strains were cultured separately in LB containing the appropriate antibiotics, subcultured and washed with PBS, as above. Strains were mixed at a 1:1 ratio immediately before gavaging 5×10^7 CFU of the mixture into the ampicillin-pre-treated mice. Faeces were monitored daily, homogenized and enumerated by selective plating. The competitive index was calculated using the ratio of population sizes of competitors at the indicated time. Mice were euthanized after seven days.

All mouse infection experiments were approved by the responsible authority (Tierversuchskommission, Kantonales Veterinäramt Zürich, license 193/2016). Sample size was not predetermined. Mouse age and gender were matched between treatment groups and animals were randomly distributed among groups. In four cases, data from mice were excluded because the mice needed to be euthanized prematurely, owing to disease or symptom severity.

Confocal microscopy. To visualize persisters in the caecum lamina propria, caecum tissues were fixed in PBS/4% paraformaldehyde, saturated in PBS/20% sucrose and embedded in optimal cutting temperature medium (OCT, Tissue-Tek) before being flash-frozen in liquid nitrogen. Ten-micrometre cryosections were air-dried, rehydrated with PBS, permeabilized with PBS/0.5%Triton X-100 and blocked with PBS/10% normal goat serum. Anti-*S.* Typhimurium LPS O5 (Difco), anti-*S.* Typhimurium LPS O12 (STA5, ref. [22]), anti-ICAM-1/CD54 (BD Biosciences), appropriate secondary antibodies, DAPI (Sigma Aldrich) and Alexa-Fluor-488-conjugated phalloidin (Santa Cruz) were used for the staining. A Zeiss Axiovert 200m microscope with 10–100× objectives, a spinning-disc confocal-laser unit (Visitron), and two Evolve 512 EMCCD cameras (Photometrics) were used for acquiring images. Images were processed using Visiview (Visitron). LPS-positive (O5-positive and/or O12-positive) *S.* Typhimurium was manually enumerated blindly in 8–12 nonconsecutive sections per mouse. Phalloidin and ICAM-1 staining were used to differentiate the lamina propria and epithelium. All data represent averages per section.

Mucus fixation and staining. Caecal tissue samples were fixed with freshly prepared Methacarn solution (60% methanol, 30% chloroform and 10% glacial acetic acid) for 24 h at room temperature[39]. The samples were transferred to methanol for 2 h and processed over night with a LogosJ tissue processor (Milestone) using the following program: 30 min, 37 °C EtOH; 30 min, 37 °C EtOH; 60 min, 37 °C EtOH; 60 min, 40 °C isopropanol, 15 min for heating up; 60 min, 45 °C isopropanol, 20 min for heating up; 180 min, 68 °C isopropanol, 20 min for heating up; and 240 min, 82 °C paraffin, 75 min for heating up.

The paraffinized tissue was then embedded as paraffin blocks for further storage. Ten-micrometre sections were deparaffinized in Xylene substitute solution (Sigma-Aldrich) for 20 min. The sections were rehydrated in sequential baths of 100%, 95%, 70%, 50% and 30% ethanol for 5 min each, and subsequently incubated for 10 min in PBS. For mucus visualization, the sections were stained with DAPI, phalloidin–FITC, wheat germ agglutinin AF647 conjugate (Invotrogen, cat. no. W32466), rabbit polyclonal anti-Salmonella O5 (Becton Dickinson, cat. no. 226601) and goat polyclonal anti-rabbit Fab Cy3 conjugate (Jackson ImmunoResearch Laboratories, cat. no. 111-167-003; RRID: AB_2313593) antibodies.

Analysis of plasmid-transfer dynamics. Mice were orally or intravenously infected with a mixture of 5 isogenic SL1344 $P2^{cat\ tag}$ strains (tags at a 1:1:1:1:1

ratio; inoculum made of approximately 10^7 CFU of each tagged strain for oral infection and 2×10^2 CFU of each tagged strain for intravenous infection) using the model protocol described in 'Oral infection model' and 'Intravenous infection model' (Figs. 1b, 2b). On day 8 (oral model), mice were gavaged with a mixture of 5 recipient strains (14028S tag, Kan^R and Amp^R; tags at 1:1:1:1:1 ratio; inoculum approximately 10^7 CFU for each tag). Barcode analysis of the recipient chromosome tags could not be performed because of technical issues with kanamycin enrichments and subsequent qPCR. In the intravenous model, the recipient used was not tagged, but was introduced on day 7 (10^8 CFU by oral gavage). The plasmid and recipient tags can be easily distinguished, as the primer pairs used for qPCR are unique (that is, WITSX-R paired with Cat_internal for P2 tags and WITSX-R paired with Kan_internal for recipient tags; in the intravenous model in which recipient tags were not used, WITSX was paired with ydgA for qPCR as there was no need for antibiotic-resistance-specific qPCR primers). For the oral model, the inocula, faeces at days 1, 9 and 15, as well as caecal tissue after gentamicin treatment, was enriched overnight in 5 ml LB containing the appropriate antibiotics (donors = streptomycin + chloramphenicol; recipients = kanamycin; and transconjugants = chloramphenicol + kanamycin) in parallel with selective plating to enumerate bacterial population sizes. For the intravenous model, the donor inoculum, as well as faeces, gall bladder, liver, spleen, mesenteric lymph nodes and caecal tissue at euthanasia (day 25) were enriched in LB with the appropriate antibiotics.

Enrichments were concentrated and genomic DNA was extracted using a QIAamp DNA Mini Kit (Qiagen). qPCR analysis was performed using temperature conditions as previously described[34]. qPCR primers are listed in Supplementary Table 2. For each sample, 5 primer pairs were used to amplify P2 tags (in the oral model WITSX-R with Cat_internal, in which X denotes 2, 11, 13, 19 or 21; in the intravenous model WITSX with ydgA in which X denotes 2, 11, 13, 19 or 21). Primers were modified from the original, previously described WITS primers[34]; tag loci remain the same as previously described[34]. Relative proportion was determined by dividing the DNA copy number (calculated from the C_T value; a dilution standard of purified chromosomal DNA allowed for a correlation between DNA copy number and C_T value) of each tag detected by the sum of all tags in the sample. The detection limit was determined by the C_T value of the most-diluted DNA standard (linearity of the standard curve decreases markedly below this value) for each qPCR run. The least-precise detection limit constitutes the conservative detection limit used for fitting our mathematical model (2.9×10^{-3}). Plasmid tags were ranked according to frequency (Extended Data Fig. 6c) as the strains are isogenic (except for the tag), and each mouse can be treated as an independent realization of the stochastic population dynamics. The data of plasmid-tag frequencies and the bacterial population counts were used to parameterize a mechanistic model of the plasmid re-seeding dynamics, and infer the most-likely rates of donor re-seeding (including initial plasmid transfer) and transconjugant-to-recipient transfer (Extended Data Fig. 6g; a detailed description is given in Supplementary Information).

Oral vaccination. Oral vaccines of *S.* Typhimurium inactivated by peracetic acid were prepared as previously described[28]. *S.* Typhimurium was grown overnight and concentrated to 10^{10} CFU/ml in PBS. Peracetic acid (Sigma-Aldrich) was added to a final concentration of 0.4% v/v, mixed vigorously and incubated at room temperature for 2 h. Traces of acid were removed after inactivation by washing bacteria with sterile PBS three times. Inactivated bacteria were resuspended at 10^{11} particles per ml in sterile PBS. Complete inactivation was ensured by inoculating a 100-μl dose of vaccine into 50 ml LB and checking for sterility. Vaccines were stored at 4 °C for up to 2 months. Mice received a 100-μl dose of vaccine by oral gavage once per week for 5 weeks. Naive control mice were mock-vaccinated with PBS.

Statistical analysis. Statistical tests on experimental data were performed using GraphPad Prism 7 for Windows. Fitting of the mathematical model to experimental values was performed using an approximate Bayesian computation approach[40]. Transfer rates were varied on a grid from 10^{-12} to 10^{-1}; the summary statistics consist of the skew of the plasmid-tag abundance distribution, the fraction of tags above the detection limit on day 15, the total size of the transconjugant population on day 15 and the time at which the transconjugant population size first exceeds 10^6 CFU per gram of faeces. A simulation is called 'successful' if all the summary statistics are within three s.d. of the experimentally observed mean of these statistics.

Ethical statement. All mouse experiments were ethically approved by the responsible authorities (Tierversuchskommission, Kantonales Veterinäramt Zürich, license 193/2016). In four cases, data from mice were excluded because the mice needed to be euthanized prematurely, owing to disease or symptom severity.

Reporting Summary. Further information on research design is available in the Nature Research Reporting Summary linked to this article.

Data availability

The genome and plasmid sequence of *E. coli* ESBL 15 have been deposited in GenBank under accession numbers CP041678–CP041681 (Biosample SAMN12275742). Numerical Source Data for all figures are provided with the paper. Source images are available upon request to the corresponding authors.

Code availability

Code for the stochastic simulation of plasmid-transfer dynamics and parameter estimation from the experimental data are provided with the paper. The R code follows the notation used in the Supplementary Information.

34. Grant, A. J. et al. Modelling within-host spatiotemporal dynamics of invasive bacterial disease. *PLoS Biol.* **6**, e74 (2008).
35. Datsenko, K. A. & Wanner, B. L. One-step inactivation of chromosomal genes in *Escherichia coli* K-12 using PCR products. *Proc. Natl Acad. Sci. USA* **97**, 6640–6645 (2000).
36. Sternberg, N. L. & Maurer, R. Bacteriophage-mediated generalized transduction in *Escherichia coli* and *Salmonella typhimurium*. *Methods Enzymol.* **204**, 18–43 (1991).
37. Stecher, B. et al. Chronic *Salmonella enterica* serovar Typhimurium-induced colitis and cholangitis in streptomycin-pretreated *Nramp1*$^{+/+}$ mice. *Infect. Immun.* **74**, 5047–5057 (2006).
38. Barthel, M. et al. Pretreatment of mice with streptomycin provides a *Salmonella enterica* serovar Typhimurium colitis model that allows analysis of both pathogen and host. *Infect. Immun.* **71**, 2839–2858 (2003).
39. Johansson, M. E. & Hansson, G. C. Preservation of mucus in histological sections, immunostaining of mucins in fixed tissue, and localization of bacteria with FISH. *Methods Mol. Biol.* **842**, 229–235 (2012).
40. Marjoram, P., Molitor, J., Plagnol, V. & Tavare, S. Markov chain Monte Carlo without likelihoods. *Proc. Natl Acad. Sci. USA* **100**, 15324–15328 (2003).
41. Zankari, E. et al. Identification of acquired antimicrobial resistance genes. *J. Antimicrob. Chemother.* **67**, 2640–2644 (2012).

Acknowledgements We thank the members of the Hardt, Slack, Bonhoeffer, Stadler and Ackermann labs for helpful discussion, and the staff at the RCHCI and EPIC animal facilities for their excellent support. This work has been funded, in part, by grants from the Swiss National Science Foundation (SNF; 310030B-173338), the Promedica Foundation, Chur and the Helmut Horten Foundation to W.-D.H., and from the SNF NFP 72 (407240-167121) to W.-D.H., S.B. and A.E. M.D. is funded by an SNF professorship grant (PP00PP_176954), E.B. by a Boehringer Ingelheim Fonds PhD fellowship, and M.E.S. and S.A.F. (in part) by the Swedish Research Council (2015-00635, 2018-02223). R.R.R. is funded by SNF grant number 31003A_179170. E.S. is supported by grant GRS 073/17 from the 'Microbials' programme of the Gebert Rüf Foundation and the SNF Bridge Discover Grant 20B2-1 180953.

Author contributions E.B. (Figs. 1, 2, 3a, b, e, f, 4, Extended Data Figs. 1–3, 4a–c, e, f, 5–9), S.A.F. (Fig. 1e, Extended Data Fig. 4a–d), A.H. (Fig. 2, Extended Data Figs. 5, 6e, f, 9e), M.F. (Extended Data Fig. 4e–h) and E.S. (Fig. 3e, f, Extended Data Fig. 7b) performed the experiments shown in the indicated figures. J.S.H., S.B. and R.R.R. (Fig. 3c, d, Extended Data Figs. 1b, 6g, 10) performed mathematical modelling shown in the indicated figures. A.E. (Extended Data Fig. 1b) provided *E. coli* strain Z2115. E.B., M.D. and W.-D.H. designed the experiments. S.A.F., M.F. and M.E.S. designed the microscopy-based experiments and analysis. E.B., M.D. and W.-D.H. conceived the project and wrote the manuscript. All authors read, commented and approved this manuscript.

Competing interests The authors declare no competing interests.

Additional information
Supplementary information is available for this paper at https://doi.org/10.1038/s41586-019-1521-8.
Correspondence and requests for materials should be addressed to M.D. or W.-D.H.
Peer review information *Nature* thanks Sophie Helaine and the other, anonymous, reviewer(s) for their contribution to the peer review of this work.
Reprints and permissions information is available at http://www.nature.com/reprints.

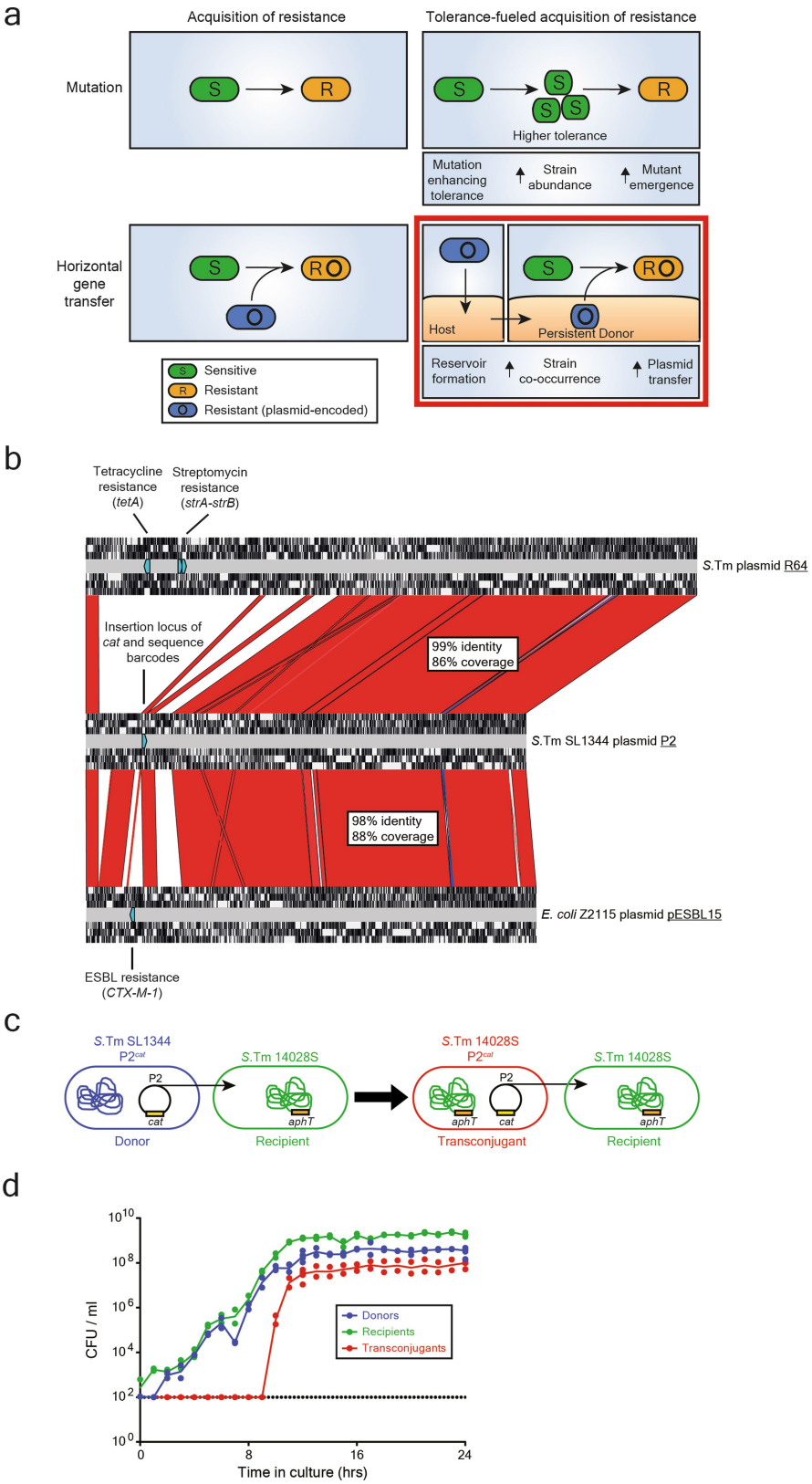

Extended Data Fig. 1 | See next page for caption.

Extended Data Fig. 1 | Emergence and spread of antibiotic resistance in bacteria using P2 as a model for conjugation. a, Antibiotic resistance in bacteria can emerge through mutation, or be acquired via horizontal gene transfer. Plasmid transfer is an important driver of the spread of antibiotic resistance. Tolerance increases the abundance of bacteria that survive antibiotic exposure, allowing for a higher probability of the emergence of mutations that lead to resistance[11]. We hypothesize that antibiotic resistance can also spread through the formation of reservoirs of persisters that contain plasmids; here, we hypothesize that the gut mucosa of the host can serve as a reservoir for persisters. The formation of long-term reservoirs, followed by re-seeding of bacteria from this reservoir into a niche occupied by other bacteria (for example, the gut lumen occupied by the microbiota following antibiotic therapy) increases the chance that two different strains interact with each other, leading to plasmid transfer (that is, increased strain co-occurrence). The representation in the bottom right panel is an example of donor persisters boosting co-occurrence. Note that tissue-associated recipient persisters may also increase co-occurrence. **b**, P2 shares homology with resistance plasmids. An alignment is shown between *S.* Typhimurium SL1344 P2 (GenBank sequence identifier HE654725.1), *S.* Typhimurium plasmid R64 (GenBank sequence identifier AP005147.1), and pESBL15 of *E. coli* Z2115 (strain isolated from a rectal swab of a patient at the University Hospital Basel) using the Artemis comparison tool (https://www.sanger.ac.uk/science/tools/artemis-comparison-tool-act). Red fill indicates high sequence identity (>85% sequence identity), blue fill indicates inversions and no fill indicates no sequence identity. For each plasmid, open reading frames (in each of the six translational frames) are shown by white regions (detected by the Artemis comparison tool). Antibiotic resistances (for example, streptomycin and tetracycline resistances on R64 and *CTX-M-1* on pESBL15) are labelled, shown by light-blue directed rectangles (found by a Basic Local Alignment Search Tool (NCBI) search against the ResFinder antibiotic-resistance-gene database[41]). In P2, the locus for insertion of the chloramphenicol-resistance cassette and neutral sequence tags is shown. For each alignment, the percentage of the sequence that aligns to P2 is shown, as well as the average sequence similarity for these regions. **c**, Model strains for addressing evolution by conjugation in *S.* Typhimurium. SL1344 contains P2^{cat} (chloramphenicol-resistance cassette (*cat*) that allows the enumeration of plasmid-bearing strains by selective plating) that can be conjugated to 14028S (kanamycin-resistance cassette (*aphT*) used for selective plating) to form a transconjugant (Cm^R and Kan^R). Transconjugants can then transfer P2^{cat} to additional recipients. **d**, P2^{cat} transfer kinetics in vitro. P2^{cat} transfer is dependent on the density of donors and recipients. Donor and recipient strains were inoculated into LB ($n = 2$, 1 experiment) at a 1:1 ratio and selective plating was performed every hour. CFUs per millilitre are reported for each population (donors in blue, recipients in green and transconjugants in red). Solid lines connect medians. The dotted line indicates the detection limit by selective plating.

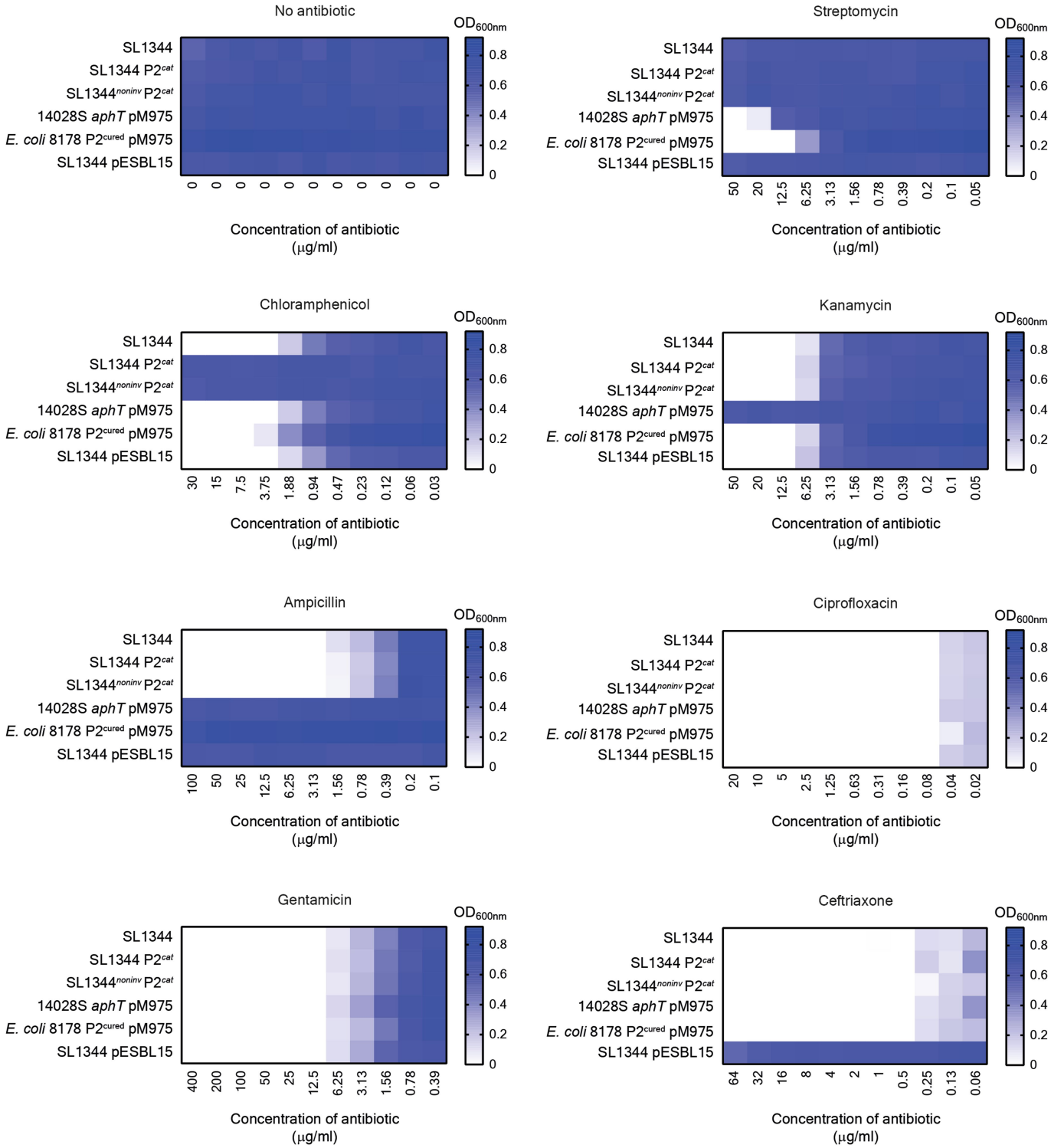

Extended Data Fig. 2 | Antibiotic-resistance profile of key strains. Antibiotic susceptibility testing was performed in LB in 96-well plates. Six strains (indicated on the figure axes) were tested against seven antibiotics, grown at 37 °C at 120 r.p.m. for 16 h, at which point the $OD_{600\ nm}$ was measured. For each antibiotic, the highest concentration used was based on the working concentration in this study. For example, the concentration of antibiotic used for selective plating in the case of streptomycin, kanamycin, ampicillin and chloramphenicol (the highest concentration of chloramphenicol was fivefold-higher than the concentration used for selective plating, because this was already close to the minimum inhibitory concentration), or the concentration of antibiotic used for the gentamicin protection assay. Importantly, a very low minimum inhibitory concentration was observed for antibiotics used in vivo to enrich for persisters (that is, ciprofloxacin and ceftriaxone). The mean of three experiments is presented on a blue–white colour gradient, in which blue indicates a large amount of bacterial growth. This is calculated by subtracting the $OD_{600\ nm}$ measured for each sample well from the background generated by the medium.

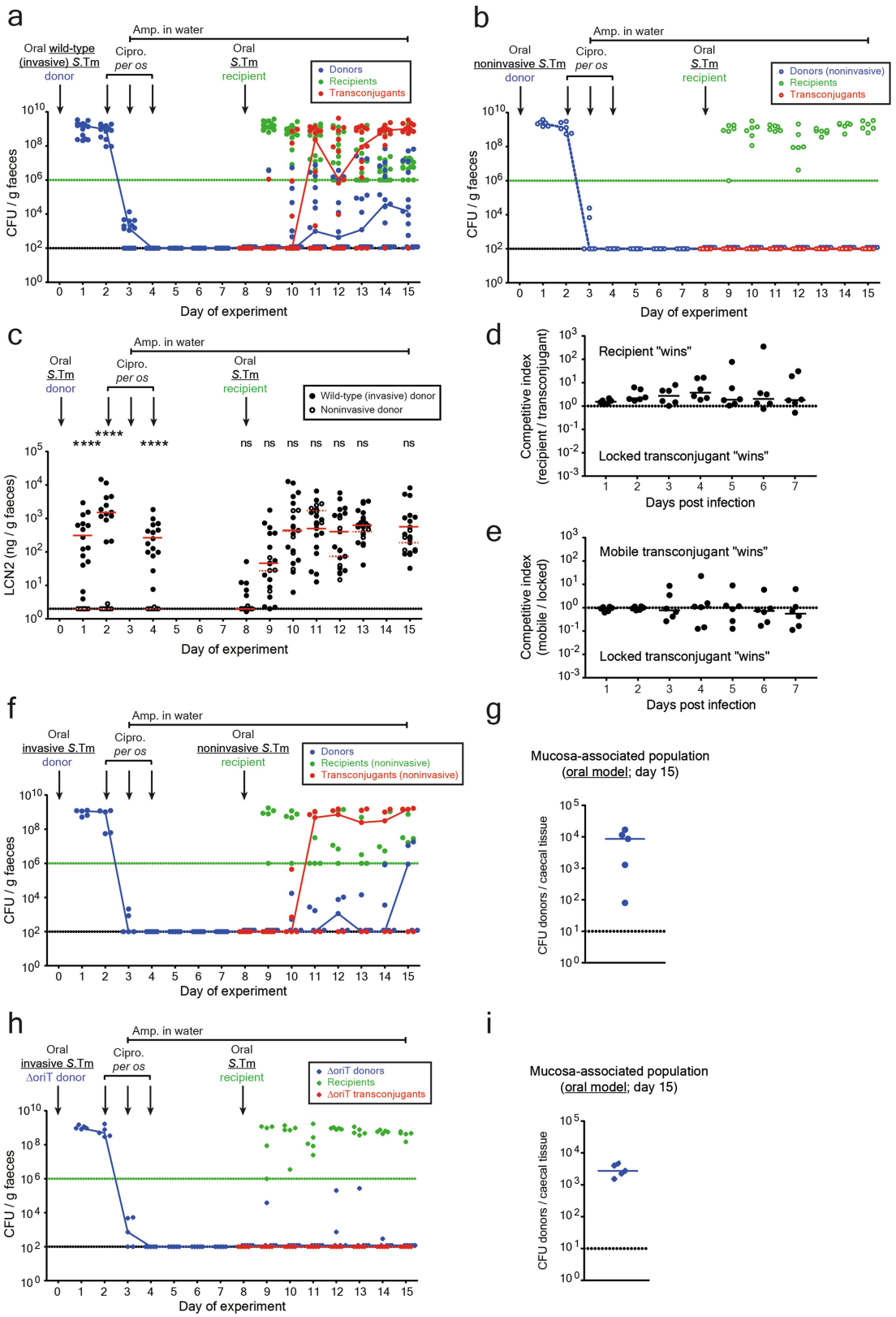

Extended Data Fig. 3 | See next page for caption.

Extended Data Fig. 3 | Controls for conjugation after antibiotic treatment in the oral infection model. a–c, Faecal bacterial-population sizes and inflammatory status of mice in Fig. 1c, d (comparison of invasive versus non-invasive donors in the oral model). Faecal loads of donors (blue, Sm^R and Cm^R), recipients (green, Kan^R), and transconjugants (red, Cm^R and Kan^R) were determined by selective plating on MacConkey agar. Black dotted line indicates detection limits for donors and transconjugants. Green dotted line indicates detection limit for recipients. The detection limit is higher for recipients once transconjugants reach a density of $>10^8$ CFU per gram of faeces. Before this happens, recipients can be found below the detection limit; the black dotted line should then be considered as the detection limit. Blue lines connect medians of donor populations; red lines connect medians of transconjugant populations. **a**, Mice infected with invasive *S*. Typhimurium donors (solid circles; $n = 15$ singly housed mice from 5 independent experiments). **b**, Mice infected with non-invasive *S*. Typhimurium donors (open circles; $n = 6$ singly housed mice from 2 independent experiments). **c**, Inflammatory status was determined by lipocalin-2 ELISA. Statistics were performed using a two-tailed Mann–Whitney *U*-test. NS, not significant ($P \geq 0.05$), $****P < 0.0001$, comparing mice infected with an invasive donor (solid black circles; $n = 15$ singly housed mice from 5 independent experiments) to mice infected with a non-invasive donor (open black circles; $n = 6$ singly housed mice from 2 independent experiments) at each time point. Medians are shown (solid red line for invasive donors; dotted red line for non-invasive donors). Dotted line indicates the detection limit. **d**, **e**, Carrying $P2^{cat}$ does not lead to a measurable fitness cost or benefit. **d**, A 'locked' transconjugant (14028S $P2^{aphT\ \Delta oriT}$ (Kan^R and Amp^R), in which conjugation is blocked by removing the origin of transfer) was competed against a recipient (14028S *cat* (Cm^R and Amp^R)). **e**, To ensure that removing the origin of transfer did not affect fitness, the locked transconjugant was competed against a transconjugant with a normal $P2^{cat}$ plasmid (that is, mobile transconjugant) (14028S $P2^{cat}$ (Cm^R and Amp^R)). In **d**, **e**, both strains were introduced at a 1:1 ratio (total inoculum size about 5×10^7 CFU per os) and faeces were monitored daily by selective plating ($n = 6$ singly housed mice from 2 independent experiments for both experiments). The competitive index is calculated by dividing the population size of one competitor by the other. Lines indicate medians. The dotted line indicates no competitive advantage for either strain. This is consistent with previously published data[20]. These data indicate that it is the plasmid-encoded conjugation efficiency (not the effects of the plasmid on host bacterial fitness) that drives the rise of transconjugants (Fig. 1c). **f**, **g**, Plasmid transfer in the oral model does not require an invasive recipient. Invasive donors (SL1344 $P2^{cat}$ (Sm^R and Cm^R)) were orally infected into pre-treated mice. After ciprofloxacin treatment, a non-invasive mutant of *S*. Typhimurium 14028S was used as a recipient (non-invasive 14028S *aphT* (Kan^R and Amp^R)). $n = 5$ mice. **f**, Selective plating determined faecal loads of donors (blue, Sm^R and Cm^R), recipients (green, Kan^R), and transconjugants (red, Cm^R and Kan^R). Black dotted line indicates the detection limit for donors and transconjugants. Green dotted line indicates the detection limit for recipients. The detection limit is higher for recipients once transconjugants reach a density of $>10^8$ CFU per gram of faeces. Before this happens, recipients can be found below the detection limit; the black dotted line should then be considered as the detection limit. Blue lines connect medians of donor populations; red lines connect medians of transconjugant populations. **g**, Donor populations enumerated after a gentamicin protection assay on caecal tissue of mice shown in **f**. Median indicated by solid line. Dotted line indicates the detection limit. **h**, **i**, Conjugation is required for plasmid transfer after antibiotic treatment. Mice were infected with invasive *S*. Typhimurium that lacks the origin of transfer in $P2^{cat}$ (SL1344 $P2^{cat\ \Delta oriT}$ (Sm^R and Cm^R)) as a donor, and 14028S *aphT* (Kan^R and Amp^R) as a recipient, after antibiotic treatment. $n = 5$ mice. **h**, Selective plating determined the faecal loads of donors (blue, Sm^R and Cm^R), recipients (green, Kan^R) and transconjugants (red, Cm^R and Kan^R). Black dotted line indicates the detection limit for donors and transconjugants. Green dotted line indicates detection limit for recipients. The detection limit is higher for recipients once transconjugants reach a density of $>10^8$ CFU per gram of faeces. Before this happens, recipients can be found below the detection limit; the black dotted line should then be considered as the detection limit. Blue lines connect medians of donor populations; red lines connect medians of transconjugant populations. **i**, Donor populations enumerated after a gentamicin protection assay on caecal tissue of mice shown in **h**. Median indicated by solid line. Dotted line indicates the detection limit.

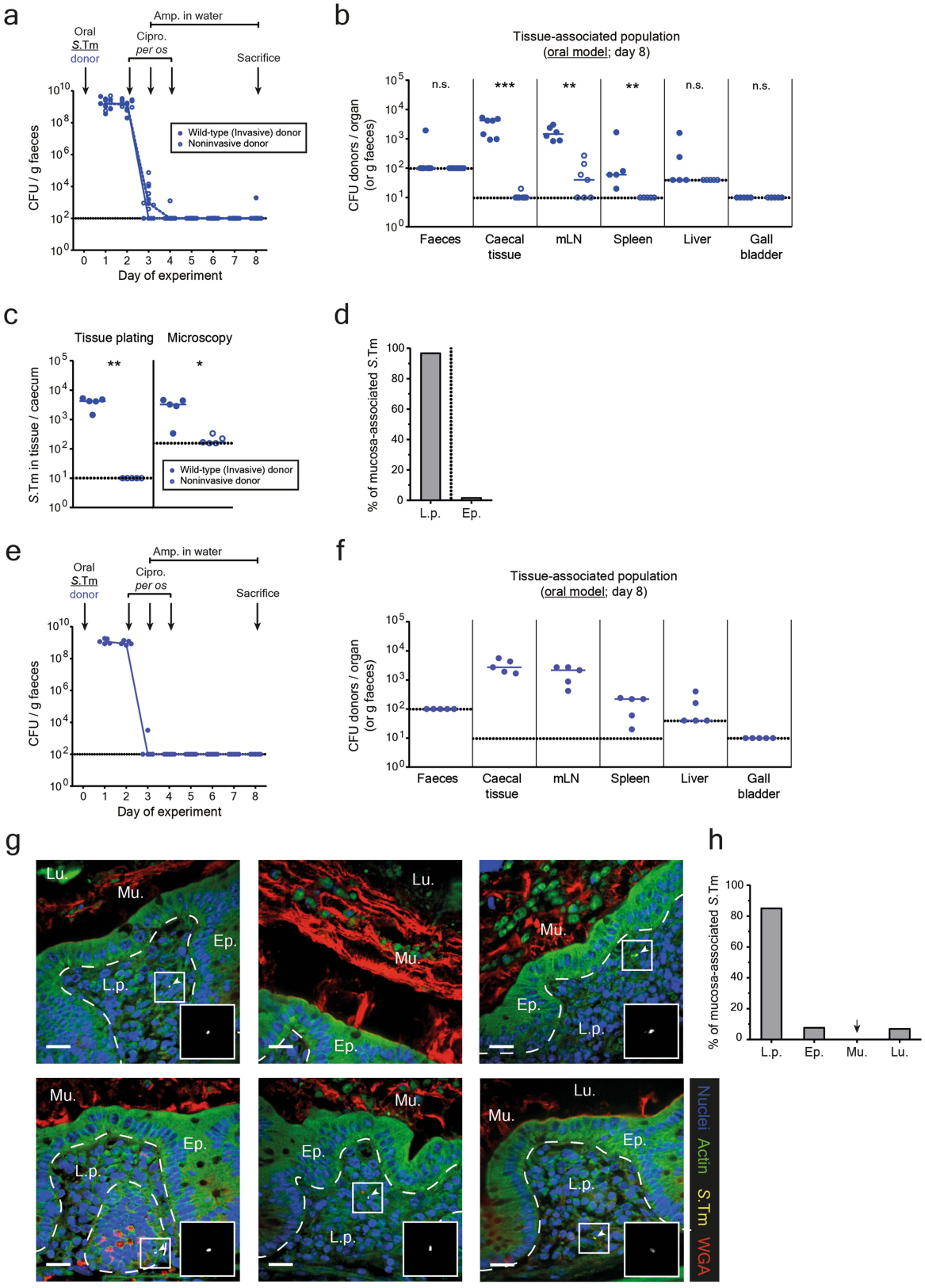

Extended Data Fig. 4 | See next page for caption.

Extended Data Fig. 4 | Quantification and localization of *S.* Typhimurium in the host mucosa after antibiotic treatments in the oral model. a–d, Mice were orally infected with either an invasive (SL1344 P2^{cat}) (blue solid circles, $n = 7$ mice) or non-invasive (non-invasive SL1344 P2^{cat}, TTSS-1 negative) (blue open circles, $n = 7$ mice) donor and treated with antibiotics. Mice were euthanized at day 8 after infection (at which point recipients were normally added), and organs were analysed. Dotted lines indicate the detection limits. **a**, Faecal populations were monitored daily by selective plating on MacConkey agar. Blue lines connect medians. **b**, Organ loads were determined by selective plating. **c**, Population size of donors in the caecal mucosa determined by selective plating after a gentamicin protection assay, or microscopy of tissue sections (same mice for each quantification method). Each data point is the average of 12 sections (10-μm thick). **b**, **c**, Statistics were performed using a two-tailed Mann–Whitney *U*-test. NS, not significant ($P \geq 0.05$), *$P < 0.05$, **$P < 0.01$, ***$P < 0.001$, ****$P < 0.0001$, comparing mice infected with invasive or non-invasive donors for each organ. **d**, Localization of *S.* Typhimurium detected in the caecal tissue by microscopy, reported as a percentage of bacteria detected in **c** in either the lamina propria (l.p.) or epithelium (ep.). Bar indicates the median from five mice. e–h, Analysis of reservoirs of persisters in Carnoy-fixed caecal tissue sections. Mice were orally infected with an invasive (SL1344 P2^{cat}, $n = 5$ mice) donor and treated with antibiotics. Mice were euthanized at day 8 after infection (at which point recipients are normally added) and organs were analysed. Dotted lines indicate the detection limits. **e**, Faecal populations were monitored daily by selective plating on MacConkey agar. Blue lines connect medians. **f**, Organ loads were determined by selective plating. Line indicates median. **g**, A Carnoy fixation was performed on caeca of mice to preserve the mucus structure. Ten-micrometre sections were stained to visualize *S.* Typhimurium (yellow, anti-LPS O5), actin (green, phalloidin–FITC), the mucus (red, wheat germ agglutinin AF647 conjugate) and nuclei (blue, DAPI). Mu., mucus. Scale bars, 20 μm. White arrows highlight *S.* Typhimurium (magnified in inset). Representative images shown from two independent experiments. **h**, Localization of *S.* Typhimurium detected in the caecal tissue by microscopy, reported as a percentage of bacteria detected each section (12 sections per mouse caecum) in the lamina propria, epithelium, mucus or lumen. Bar indicates the median from five mice.

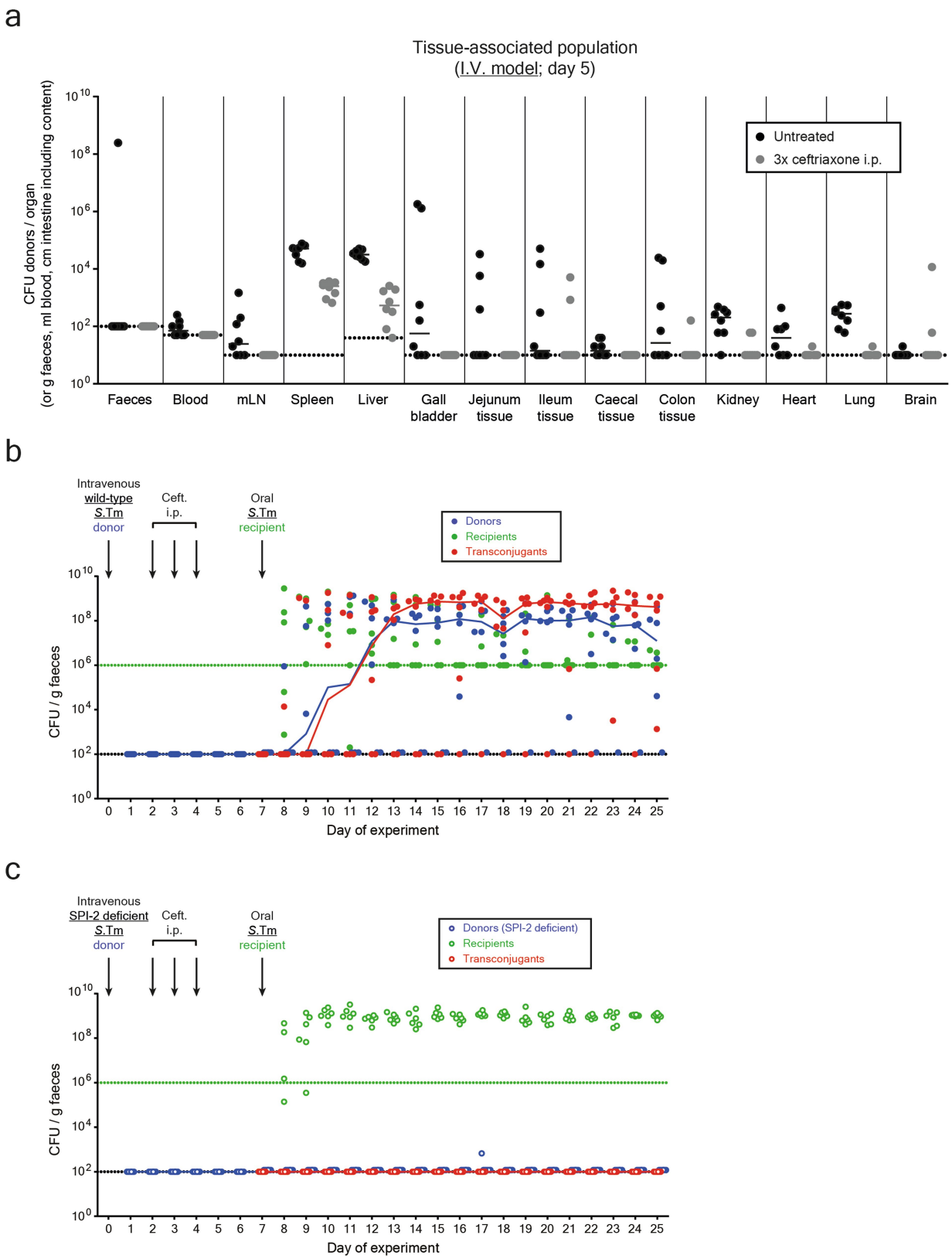

Extended Data Fig. 5 | See next page for caption.

Extended Data Fig. 5 | Determination of reservoirs of tissue-associated persisters after intravenous infection, and subsequent plasmid transfer. **a**, An equal mix of five SL1344 P2$^{cat\ tag}$ strains (Sm^R and Cm^R) were intravenously infected into mice (10^3 CFU). Treatments were as described in Fig. 2b (grey circles, 3 intraperitoneal doses of ceftriaxone; $n = 8$ singly housed mice from 2 independent experiments) or mice were left untreated (black circles; $n = 8$ singly housed mice from 2 independent experiments). Mice were euthanized on day 5 of the experiment (after the final dose of ceftriaxone was given). The tissue-associated populations in organs were enumerated by selective plating. Detection limit by selective plating is shown as a dotted line. Lines indicate median. **b**, **c**, Faecal bacterial population sizes of mice in Fig. 2d, e (comparison of wild-type and SPI-2-negative donors in the intravenous model). Faecal loads of donors (blue, Sm^R and Cm^R), recipients (green, Kan^R) and transconjugants (red, Cm^R and Kan^R) were determined by selective plating on MacConkey agar. Black dotted line indicates the detection limits for donors and transconjugants. Green dotted line indicates the detection limit for recipients. The detection limit is higher for recipients once transconjugants reach a density of $>10^8$ CFU per gram of faeces. Before this happens, recipients can be found below the detection limit; the black dotted line should then be considered as the detection limit. Blue lines connect medians of donor populations; red lines connect medians of transconjugant populations. **b**, Mice infected with wild-type *S.* Typhimurium donors (solid circles). **c**, Mice infected with SPI-2-deficient *S.* Typhimurium donors (open circles).

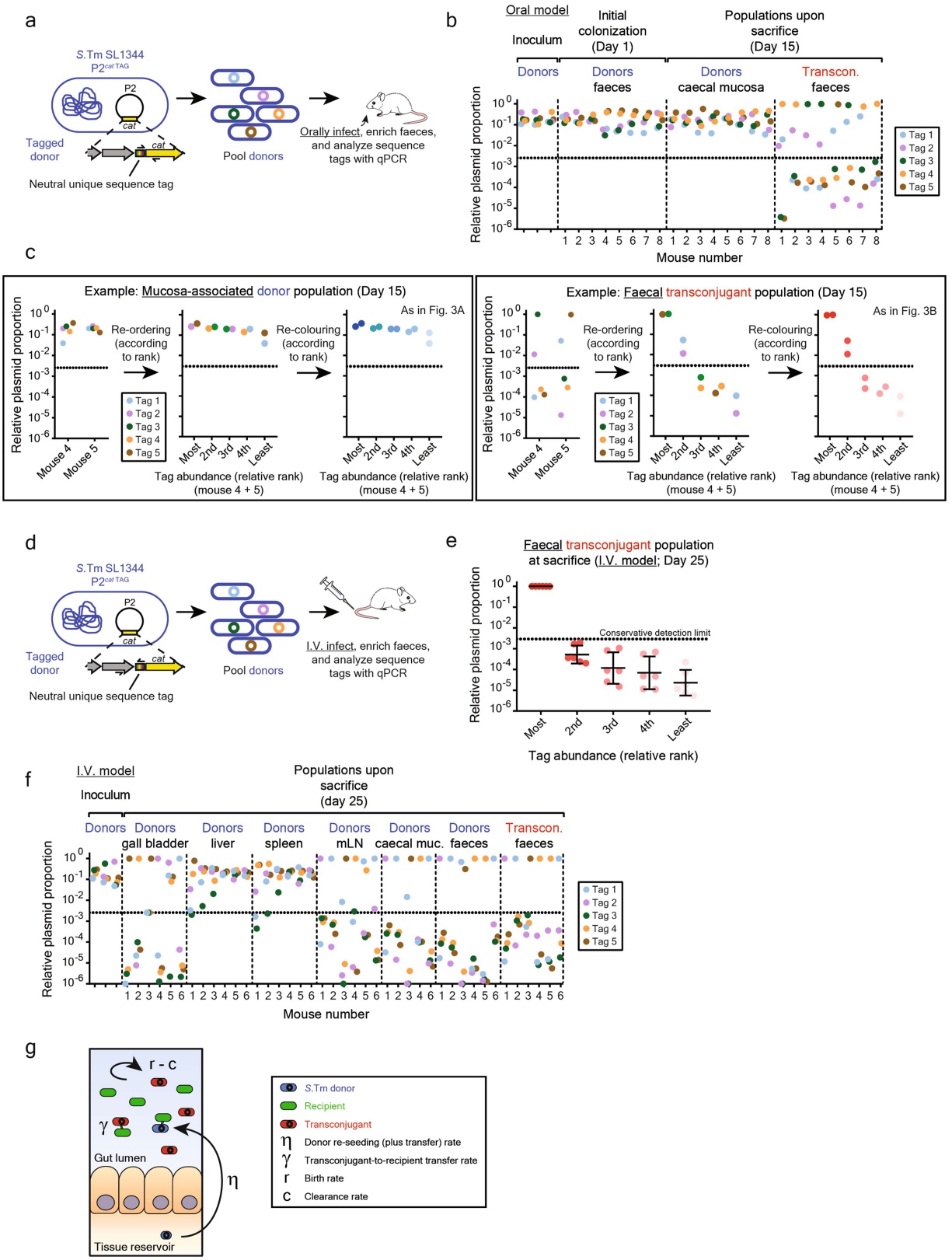

Extended Data Fig. 6 | See next page for caption.

Extended Data Fig. 6 | Experimental strategy for assessing population dynamics and tag frequencies. Relates to Fig. 3a–d. **a**–**c**, Tags introduced in the oral model. **a**, Tags coupled to a chloramphenicol-resistance cassette were introduced in P2. qPCR primers are specific to the chloramphenicol-resistance cassette and the specific tag (shown as one-sided arrows). Five tagged donors were pooled and orally infected as a 1:1:1:1:1 mix into mice. **b**, Relative plasmid-tag proportion detected by qPCR in the initial donor population, the donor population persisting in the caecal mucosa and the transconjugant population is shown for eight mice (three independent inocula). Dotted line indicates the detection limit. Each tag is given a unique colour. **c**, Scheme illustrating how tags were sorted and recoloured to yield the plots in Fig. 3a, b. Two mice are shown as examples. For the mucosa-associated donor populations (top) and for the faecal transconjugant populations (bottom), tags were sorted according to relative frequency. These tags were re-coloured (darker colour indicates higher frequency) to visualize the trends shown in Fig. 3a, b. These re-ordered tags were used as the experimental data for fitting the mathematical model. **d**–**f**, Experimental strategy to assess plasmid-transfer dynamics in the intravenous model. **d**, Tags coupled to a chloramphenicol-resistance cassette were introduced in P2. qPCR primers are specific to *ydgA* (a pseudogene flanking the specific tags) and the specific tag (shown as one-sided arrows). Five tagged donors were pooled and intravenously infected as a 1:1:1:1:1 mix into mice. **e**, Tags from the faecal transconjugant population at day 25 are sorted by abundance. Note that each abundance rank can consist of any tag (ranking and re-colouring scheme in **c** and raw tag data in **f**). $n = 6$ singly housed mice from 2 independent experiments. Dotted line indicates the conservative detection limit by qPCR. This detection limit refers to the most-conservative detection limit of any qPCR run (2.9×10^{-3}; that is, tags can appear below this detection limit if the qPCR run yielded a lower detection limit). Line indicates the mean; error bars indicate the s.d. **f**, Relative plasmid-tag proportion detected by qPCR in the inoculum, the donor population persisting in the internal organs and the transconjugant population in the faeces is shown for six mice (three independent inocula; faeces and organ population data in Fig. 2d). Dotted line indicates the detection limit. Each tag is given a unique colour. **g**, Representation of key parameters in the mathematical model. Donors form a reservoir of persisters in host tissues. These cells can interact with other bacteria that colonize the gut lumen (that is, recipients), and transfer plasmids. Our mathematical model summarizes these plasmid-transfer dynamics using a few key parameters. Donors re-seed the gut lumen and transfer plasmids at rate η, transconjugants transfer plasmids to recipients (without a plasmid) at rate γ and the turn-over of each bacterial population is given by $r - c$, in which r is the birth rate and c is the clearance rate.

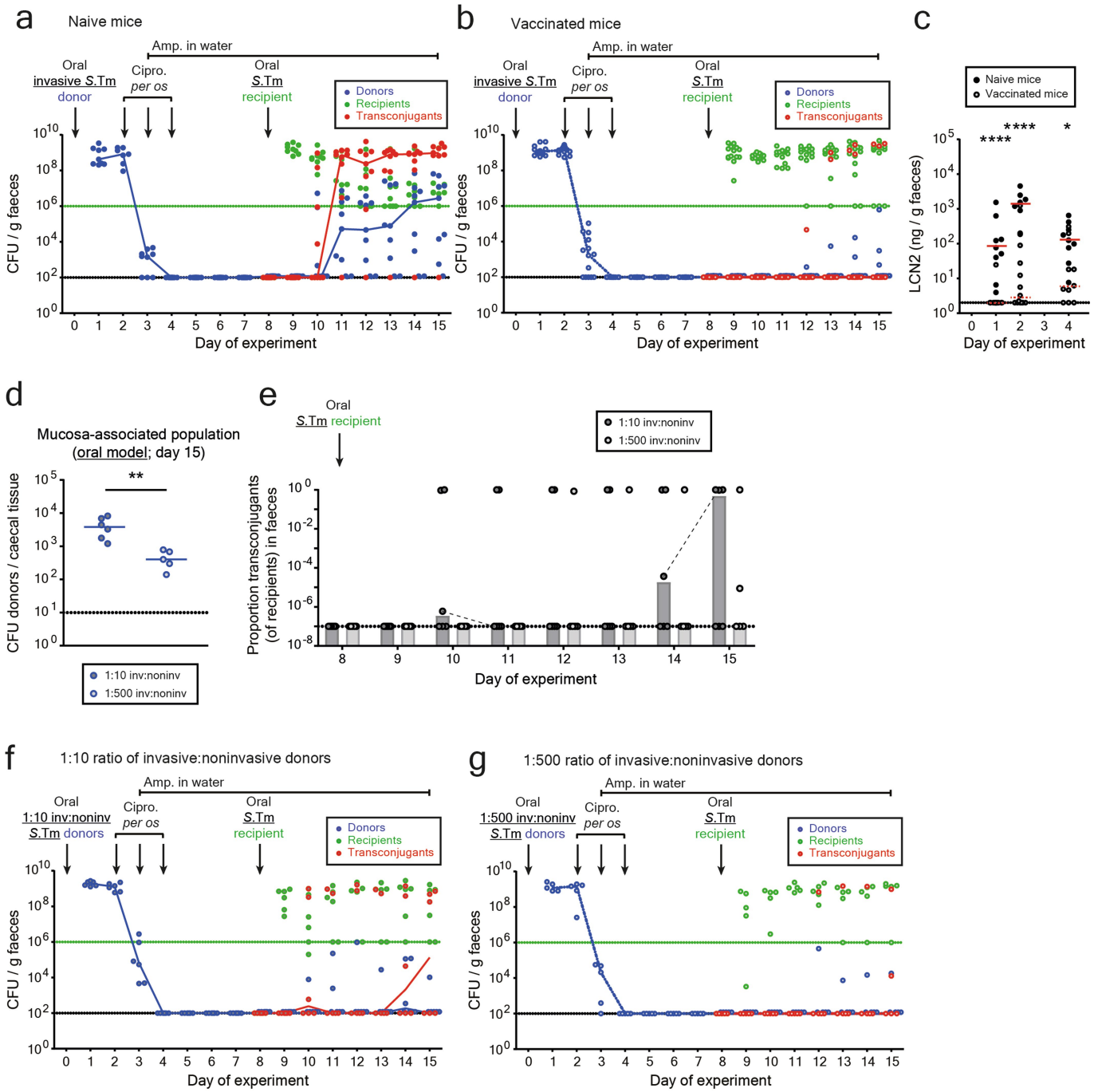

Extended Data Fig. 7 | See next page for caption.

Extended Data Fig. 7 | Faecal bacterial-population sizes and inflammatory status of mice (comparison of vaccinated versus naive mice in the oral model), and validation by mixtures of invasive and non-invasive donors. Relates to Fig. 3e, f. **a**, **b**, Faecal loads of donors (blue, Sm^R and Cm^R), recipients (green, Kan^R), and transconjugants (red, Cm^R and Kan^R) were determined by selective plating on MacConkey agar. Barcode analysis of the recipient chromosome tags could not be performed because of technical issues with kanamycin enrichments and subsequent qPCR. Black dotted lines indicate the detection limits for donors and transconjugants. Green dotted line indicates the detection limit for recipients. The detection limit is higher for recipients once transconjugants reach a density of $>10^8$ CFU per gram of faeces. Before this happens, recipients can be found below the detection limit; the black dotted line should then be considered as the detection limit. Blue lines connect medians of donor populations; red lines connect medians of transconjugant populations. **a**, Naive mice infected with invasive *S.* Typhimurium donors (solid circles). **b**, Vaccinated mice infected with invasive *S.* Typhimurium donors (open circles with light-grey fill). **c**, Inflammatory status to determine the success of vaccination was determined by lipocalin-2 ELISA. Statistics were performed using a two-tailed Mann–Whitney *U*-test. NS, not significant ($P \geq 0.05$), $^*P < 0.05$, $^{**}P < 0.01$, $^{***}P < 0.001$, $^{****}P < 0.0001$, comparing naive mice (black circles, $n = 9$ singly housed mice from 3 independent experiments) to vaccinated mice (open circles, $n = 14$ singly housed mice from 4 independent experiments) at each time point. Medians are shown (solid red line for naive mice and dotted red line for vaccinated mice). Dotted line the indicates detection limit. **d**–**g**, Experimentally reducing the population size of mucosa-associated persisters by mixing invasive and non-invasive donors reduces plasmid transfer in the oral model. Mice were orally infected with a mixture of invasive (SL1344 $P2^{cat}$, Sm^R and Cm^R) and non-invasive (non-invasive SL1344 $P2^{cat}$, Sm^R and Cm^R) donors at two ratios: 1:10 ($n = 6$ singly housed mice) or 1:500 ($n = 5$ singly housed mice). In both cases, an excess of non-invasive donors was used to experimentally reduce the number of cells that can establish a reservoir of persisters in the intestinal mucosa (two independent experiments). *S.* Typhimurium 14028S *aphT* (Kan^R and Amp^R) was used as a recipient after antibiotic treatment. **d**, Donor populations enumerated after a gentamicin protection assay on caecal tissue of mice infected with a 1:10 ratio (blue circles with dark grey fill; line indicates median) or 1:500 ratio (blue circles with light grey fill; line indicates median) of invasive to non-invasive donors. Statistics were performed using a two-tailed Mann–Whitney *U*-test $^{**}P < 0.01$. **e**, Proportion of transconjugants (transconjugant population size divided by the sum of recipients and transconjugants) in the faeces is shown for each day, for mice infected with a 1:10 ratio (black circles with dark grey fill, grey bars indicate median) or a 1:500 ratio (black circles with light grey fill, light grey bars indicate median) of invasive to non-invasive donors. **f**, **g**, Faecal loads of donors (blue, Sm^R and Cm^R), recipients (green, Kan^R) and transconjugants (red, Cm^R and Kan^R) were determined by selective plating on MacConkey agar. **f**, Mice infected with a 1:10 ratio of invasive to non-invasive donors. **g**, Mice infected with a 1:500 ratio of invasive to non-invasive donors. In **d**–**g**, the black dotted line indicates the detection limit for donors and transconjugants. Green dotted line indicates the detection limit for recipients. The detection limit is higher for recipients once transconjugants reach a density of $>10^8$ CFU per gram of faeces. Before this happens, recipients can be found below the detection limit; the black dotted line should then be considered as the detection limit.

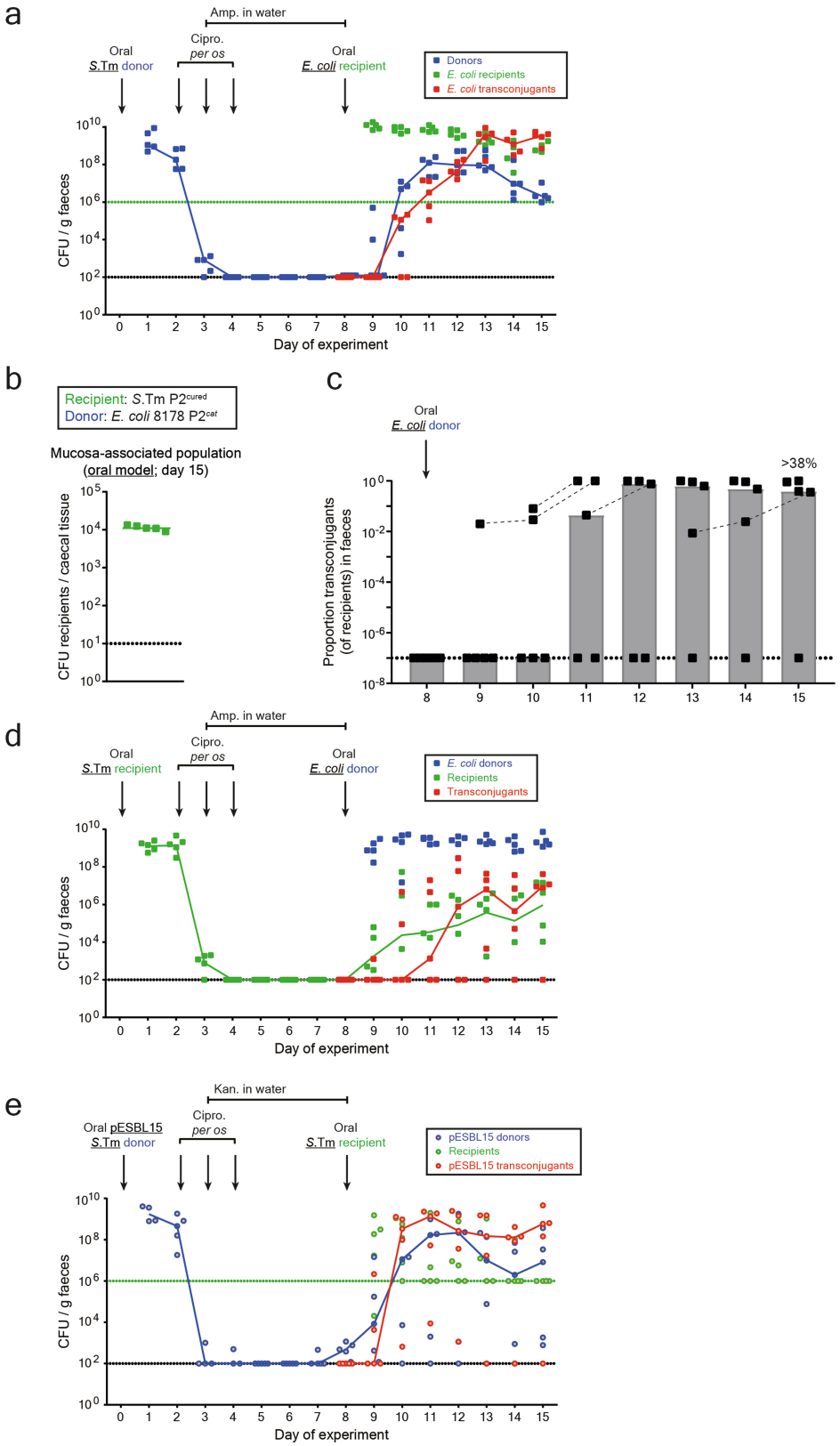

Extended Data Fig. 8 | See next page for caption.

Extended Data Fig. 8 | Faecal bacterial-population sizes of mice and the role of persistence and conjugation in host tissues if the recipient constitutes the reservoir. Relates to Fig. 4. **a**, Faecal loads of donors (blue, Sm^R and Cm^R), recipients (green, Amp^R), and transconjugants (red, Cm^R and Amp^R) were determined by selective plating on MacConkey agar (same mice as in Fig. 4a, b; *S.* Typhimurium donor and *E. coli* recipient in the oral model). Black dotted line indicates the detection limit for donors and transconjugants. Green dotted line indicates the detection limit for recipients. The detection limit is higher for recipients once transconjugants reach a density of $>10^8$ CFU per gram of faeces. Before this happens, recipients can be found below the detection limit; the black dotted line should then be considered as the detection limit. Blue lines connect medians of donor populations; red lines connect medians of transconjugant populations. **b**–**d**, Persistence in host tissues also promotes plasmid transfer if the recipient constitutes the reservoir. Pre-treated mice were orally infected with a *S.* Typhimurium recipient (SL1344 $P2^{cured}$ *aphT*, Sm^R and Kan^R) and treated with ciprofloxacin and ampicillin as in the oral model (Fig. 1b). On day 8, ampicillin was removed from the drinking water and an *E. coli* donor was introduced orally (*E. coli* 8178 $P2^{cat}$, Cm^R and Amp^R). **b**, Recipient populations enumerated after a gentamicin protection assay on caecal tissue ($n = 5$ singly housed mice from 2 independent experiments). Line indicates median. **c**, Proportion of transconjugants (transconjugant population size divided by sum of recipients and transconjugants) in the faeces is shown for each day. Grey bars indicate median. **d**, Faecal loads of recipients (green, Sm^R and Kan^R), donors (blue, Cm^R and Amp^R), and transconjugants (red, Sm^R, Cm^R and Kan^R) were determined by selective plating on MacConkey agar. In **b**–**d**, dotted lines indicate detection limits by selective plating. **e**, Faecal bacterial-populations sizes of mice in Fig. 4c, d (*S.* Typhimurium ESBL donor in the oral model). Faecal loads of donors (blue, Sm^R and Amp^R), recipients (green, Kan^R) and transconjugants (red, Kan^R and Amp^R) were determined by selective plating on MacConkey agar. Black dotted line indicates the detection limit for donors and transconjugants. Green dotted line indicates the detection limit for recipients. The detection limit is higher for recipients once transconjugants reach a density of $>10^8$ CFU per gram of faeces. Before this happens, recipients can be found below the detection limit; the black dotted line should then be considered as the detection limit. Blue lines connect medians of donor populations; red lines connect medians of transconjugant populations.

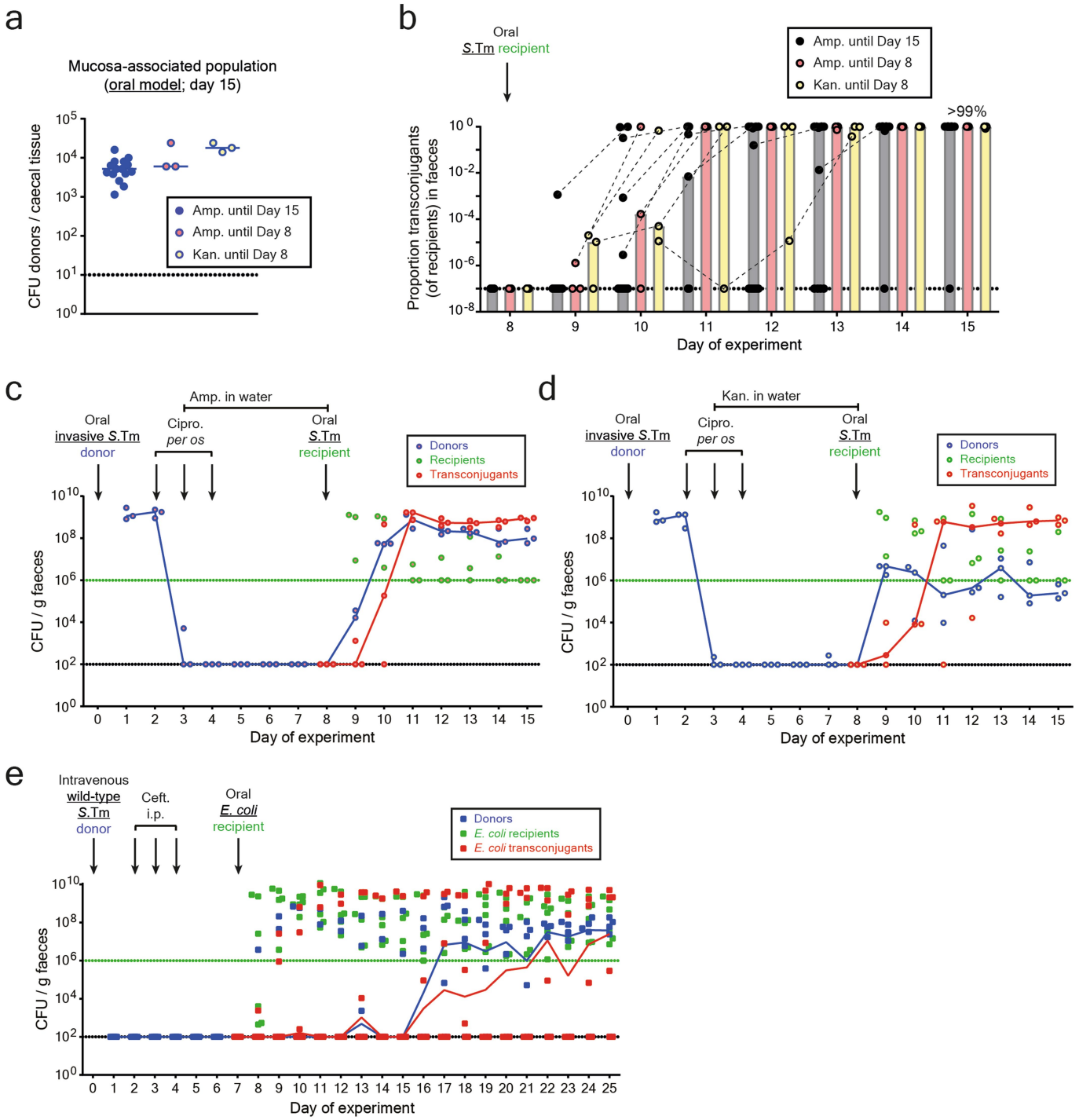

Extended Data Fig. 9 | See next page for caption.

Extended Data Fig. 9 | Exchanging ampicillin for kanamycin to limit gut-luminal growth of the donor does not affect the overall plasmid-transfer kinetics, and faecal bacteria-population sizes of intravenously infected mice. Relates to Fig. 4. **a**–**d**, Mice were orally infected with SL1344 P2^{cat} (Sm^R and Cm^R) as a donor, and 14028S *aphT* (Kan^R and Amp^R) as a recipient after antibiotic treatment. Mice were either treated with ampicillin in the drinking water until day 15 (normal protocol as in Fig. 1b), day 8 (when the recipient is added) or kanamycin until day 8. **a**, Donor populations enumerated after a gentamicin protection assay on caecal tissue of mice, in which ampicillin is maintained until day 15 (solid blue circles, $n = 15$ singly housed mice from 5 independent experiments; data taken from Fig. 1d), ampicillin is removed on day 8 (blue circles with pink fill, $n = 3$ singly housed mice from 1 experiment) or kanamycin is used until day 8 (blue circles with yellow fill, $n = 3$ singly housed mice from 1 experiment). Median indicated by solid line. **b**, Proportion of transconjugants (transconjugant population size divided by the sum of recipients and transconjugants) is shown for the groups receiving ampicillin treatment until day 15 (solid black circles, grey bars indicate median; $n = 15$ singly housed mice from 5 independent experiments; data taken from Fig. 1c), ampicillin treatment until day 8 (black circles with pink fill, pink bars indicate median; $n = 3$ singly housed mice from 1 experiment), and kanamycin treatment until day 8 (black circles with yellow fill, yellow bars indicate median; $n = 3$ singly housed mice from 1 experiment). **c**, **d**, Faecal loads of donors (blue, Sm^R and Cm^R), recipients (green, Kan^R) and transconjugants (red, Cm^R and Kan^R) were determined by selective plating on MacConkey agar. **c**, Mice treated until day 8 with ampicillin. **d**, Mice treated until day 8 with kanamycin. In **a**–**d**, the black dotted line indicates the detection limit for donors and transconjugants. Green dotted line indicates the detection limit for recipients. The detection limit is higher for recipients once transconjugants reach a density of $>10^8$ CFU per gram of faeces. Before this happens, recipients can be found below the detection limit; the black dotted line should then be considered as the detection limit. **e**, Faecal bacterial-populations sizes of mice in Fig. 4e, f (*S.* Typhimurium donor and *E. coli* recipient in the intravenous model). Faecal loads of donors (blue, Sm^R and Amp^R), recipients (green, Kan^R) and transconjugants (red, Kan^R and Amp^R) were determined by selective plating on MacConkey agar. Black dotted line indicates the detection limit for donors and transconjugants. Green dotted line indicates the detection limit for recipients. The detection limit is higher for recipients once transconjugants reach a density of $>10^8$ CFU per gram faeces. Before this happens, recipients can be found below the detection limit; the black dotted line should then be considered as the detection limit. Blue lines connect medians of donor populations; red lines connect medians of transconjugant populations.

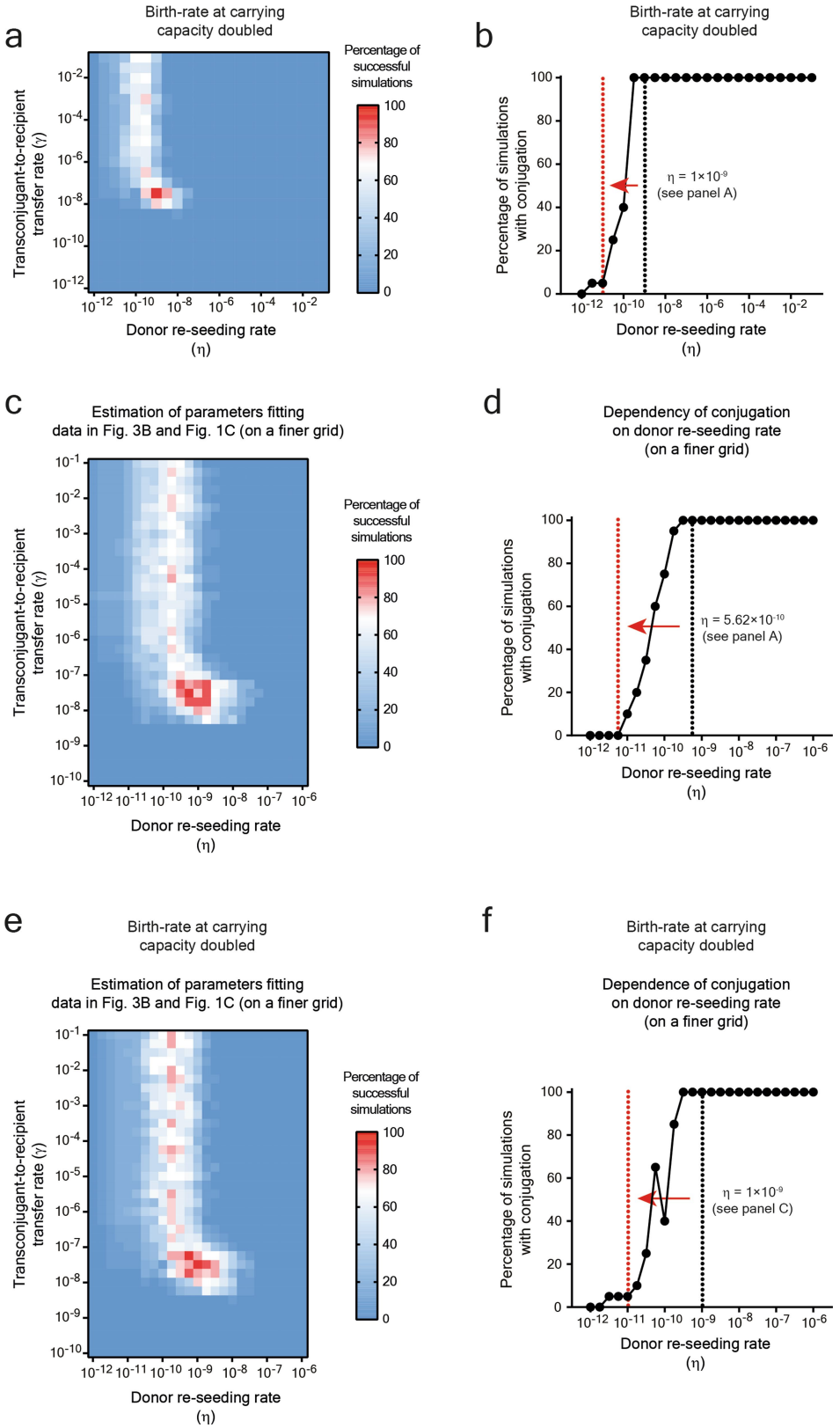

Extended Data Fig. 10 | See next page for caption.

Extended Data Fig. 10 | Increasing growth rate at carrying capacity to model inflammation, or running simulations on a finer parameter grid, does not affect overall simulation trends. a, **b**, Simulations were run with identical parameters to Fig. 3c, d, but an increased birth and death rate at carrying capacity to simulate cases in which inflammation is present (Supplementary Information). The trends of the simulations remain the same as in Fig. 3c, d. **a**, Likelihood of the model as a function of the donor re-seeding (including donor-to-recipient conjugation) rate, and the rate of transconjugant-to-recipient plasmid transfer. All other parameter values are given in the Supplementary Information. The most-likely set of parameters is shown in red ($\eta = 1 \times 10^{-9}$ events per recipient per day; $\gamma = 3.16 \times 10^{-8}$ events per recipient per CFU per gram of faeces per day). **b**, The fraction of simulations with plasmid re-seeding (defined as a final transconjugant population size above 5×10^{8} CFU per gram of faeces) is shown as a function of η. Here, γ is fixed at its most-likely value of 3.16×10^{-8} events per recipient per CFU per gram of faeces per day. The black vertical dotted line at $\eta = 1 \times 10^{-9}$ events per recipient per day indicates the estimated most-likely value from **a**. The red vertical dotted line at $\eta = 1 \times 10^{-11}$ events per recipient per day indicates a hypothetical 100-fold decrease of η (shown by a red arrow) (as might be caused, for example, by vaccination). **c**–**f**, Running simulations on a finer parameter grid does not affect the overall simulation trends. Supplementary Table 4 provides details of the differences between specific simulation results. **c**, **d**, Simulations were run on a grid of $\eta = 10^{-12}$ to 10^{-6} and $\gamma = 10^{-10}$ to 10^{-1} with 0.25-log increments, instead of the $\eta = 10^{-12}$ to 10^{-1} and $\gamma = 10^{-12}$ to 10^{-1} with 0.5-log increments used in Fig. 3c, d. **e**, **f**, Simulations were run with parameters identical to **a**, **b**, but on a grid of $\eta = 10^{-12}$ to 10^{-6} and $\gamma = 10^{-10}$ to 10^{-1} with 0.25-log increments, instead of $\eta = 10^{-12}$ to 10^{-1} and $\gamma = 10^{-12}$ to 10^{-1} with 0.5-log increments. **c**, **e**, Likelihood of the model as a function of the donor re-seeding (including donor-to-recipient conjugation) rate, and the rate of transconjugant-to-recipient plasmid transfer. All other parameter values are given in the Supplementary Information. The most-likely set of parameters is shown in red. **d**, **f**, The fraction of simulations with plasmid re-seeding (defined as a final transconjugant population size above 5×10^{8} CFU per gram of faeces) is shown as a function of η. Here γ is fixed at its most likely value. The black vertical dotted line indicates the estimated most-likely value (from **c** or **e**). The red vertical dotted line indicates a hypothetical 100-fold decrease of η (shown by a red arrow) (as might be caused, for example, by vaccination).

Corresponding author(s): Wolf-Dietrich Hardt
Mederic Diard

Reporting Summary

Nature Research wishes to improve the reproducibility of the work that we publish. This form provides structure for consistency and transparency in reporting. For further information on Nature Research policies, see Authors & Referees and the Editorial Policy Checklist.

Statistical parameters

When statistical analyses are reported, confirm that the following items are present in the relevant location (e.g. figure legend, table legend, main text, or Methods section).

n/a	Confirmed	
☐	☒	The exact sample size (*n*) for each experimental group/condition, given as a discrete number and unit of measurement
☐	☒	An indication of whether measurements were taken from distinct samples or whether the same sample was measured repeatedly
☐	☒	The statistical test(s) used AND whether they are one- or two-sided *Only common tests should be described solely by name; describe more complex techniques in the Methods section.*
☐	☒	A description of all covariates tested
☐	☒	A description of any assumptions or corrections, such as tests of normality and adjustment for multiple comparisons
☐	☒	A full description of the statistics including central tendency (e.g. means) or other basic estimates (e.g. regression coefficient) AND variation (e.g. standard deviation) or associated estimates of uncertainty (e.g. confidence intervals)
☐	☒	For null hypothesis testing, the test statistic (e.g. *F*, *t*, *r*) with confidence intervals, effect sizes, degrees of freedom and *P* value noted *Give P values as exact values whenever suitable.*
☐	☒	For Bayesian analysis, information on the choice of priors and Markov chain Monte Carlo settings
☒	☐	For hierarchical and complex designs, identification of the appropriate level for tests and full reporting of outcomes
☒	☐	Estimates of effect sizes (e.g. Cohen's *d*, Pearson's *r*), indicating how they were calculated
☐	☒	Clearly defined error bars *State explicitly what error bars represent (e.g. SD, SE, CI)*

Our web collection on statistics for biologists may be useful.

Software and code

Policy information about availability of computer code

Data collection	Data collection is described in detail in Materials and Methods. The mathematical model is described in detail in the supplementary materials. All code needed to reproduce the mathematical modelling is available as supplementary data. The custom code was written in R, and tested on MacOS 10.13.4 with R 3.4.4, as well as a computing cluster running CentOS 7 with R 3.4.0. There is an essential dependence on the R package adaptivetau (v2.2.1); and optional dependencies on the packages ggplot2 (v2.2.1), reshape2 (v1.4.3), gridExtra (v2.3), wesanderson (v0.3.6), parallel (v3.4.4), and tictoc (v1.0).
Data analysis	Statistical analysis and computation of the plots was performed using Graph Pad Prism, version 7; Fitting of the mathematical model to experimental values was performed using an Approximate Bayesian Computation (ABC) approach (the reference Marjoram et al. 2003, PNAS describes this in detail).

For manuscripts utilizing custom algorithms or software that are central to the research but not yet described in published literature, software must be made available to editors/reviewers upon request. We strongly encourage code deposition in a community repository (e.g. GitHub). See the Nature Research guidelines for submitting code & software for further information.

Data

Policy information about availability of data

All manuscripts must include a data availability statement. This statement should provide the following information, where applicable:

- Accession codes, unique identifiers, or web links for publicly available datasets
- A list of figures that have associated raw data
- A description of any restrictions on data availability

All data from experiments and from the mathematical model calculations are shown. The sequence data is available at the indicated repositories (accession number is provided in the data availability statement).

Field-specific reporting

Please select the best fit for your research. If you are not sure, read the appropriate sections before making your selection.

☐ Life sciences ☐ Behavioural & social sciences ☒ Ecological, evolutionary & environmental sciences

For a reference copy of the document with all sections, see nature.com/authors/policies/ReportingSummary-flat.pdf

Ecological, evolutionary & environmental sciences study design

All studies must disclose on these points even when the disclosure is negative.

Study description	We performed mouse infection experiments. The numbers of mice per group are indicated in each figure. In figures where statistical comparisons were performed, we used a minimum of 5 mice that were singly housed per group (to ensure that each mouse is truly independent) per group from at least two independent experiments. In other experiments, we used a minimum of three singly housed mice per group. We sampled feces at the indicated times post infection and analyzed pathogens loads in tissues by plating and by fluorescence microscopy.
Research sample	We used defined clones of the indicated S. Typhimurium and E. coli strains. 8-12 weeks old 129 SvEv (Nramp+/+) inbred mice were used. The Nramp+/+ genotype confers resistance against long-term S. Typhimurium infection. The mice harbor a specified pathogen free microbiota. This resident microbiota does not feature any E. coli or Salmonella strains.
Sampling strategy	We sampled feces at the indicated times post infection and analyzed pathogens loads in tissues by plating and by fluorescence microscopy. Sample sizes were not predetermined. As large differences were expected, 5-7 mice were used in general for statistical comparisons. In some cases where the underlying data was central to the main hypothesis, we used as many as 15 mice to ensure claims were accurate and that we encompasses as large variability as possible.
Data collection	We sampled feces at the indicated times post infection and analyzed pathogens loads in tissues by plating and by fluorescence microscopy. Data was recorded by the experimenter (indicated in the author contributions section).
Timing and spatial scale	The time course of the sampling is shown in detail in Figure 1B and Figure 2B. Mice were infected and feces were monitored daily for either 5, 7, 8, 15, or 25 days (indicated for each figure specifically). Antibiotic treatments were given on days 2, 3, and 4 (where applicable). Organs were collected at defined endpoints in the experiment.
Data exclusions	All experimental data from all repeat of each experiment is shown. We did not exclude any data, except in the case of four mice where animals needed to be sacrificed prematurely due to disease or symptom severity.
Reproducibility	The number of animals used in the independent experiments are indicated in the figure legends. Mice were singly housed to ensure that each sample is completely independent. Experiments were very reproducible in each independently housed mouse. In addition, in the bulk majority of experiments, at least two independent experiments (with separate inocula) were used to validate reproducibility.
Randomization	Mice were randomly assigned to the different experimental groups.
Blinding	The data analysis was not performed in a blinded fashion. This is explained by the objective nature of the plating data (colony present = yes/no), which excludes enumeration bias. For microscopy, slides were blinded prior to analysis.

Did the study involve field work? ☐ Yes ☒ No

Reporting for specific materials, systems and methods

Materials & experimental systems

n/a	Involved in the study
[ ]	[x] Unique biological materials
[ ]	[x] Antibodies
[x]	[ ] Eukaryotic cell lines
[x]	[ ] Palaeontology
[ ]	[x] Animals and other organisms
[x]	[ ] Human research participants

Methods

n/a	Involved in the study
[x]	[ ] ChIP-seq
[x]	[ ] Flow cytometry
[x]	[ ] MRI-based neuroimaging

Unique biological materials

Policy information about availability of materials

Obtaining unique materials	All materials are freely available from public repositories or commercial suppliers. The unique strains and plasmid constructs created for the plasmid transfer experiments are available from the corresponding author (W.D. Hardt).

Antibodies

Antibodies used	α-S.Tm LPS O12 monoclonal antibody (STA5; (reference Moor et al. 2017, Nature, dil. 1:200)), α-ICAM-1/CD54 antibody (BD Biosciences, Cat# 553250, dil. 1:100), DAPI (Sigma Aldrich, Cat# D9542, 0.1 µg/ml), AlexaFluor488-conjugated phalloidin (Santa Cruz, sc-363791, dil. 1:200), wheat germ agglutinin (WGA) AF647 conjugate (Invitrogen, Cat#W32466, dil. 1:200), Rabbit polyclonal anti-Salmonella O5 (Becton Dickinson, Cat#226601, dil. 1:200) and Goat polyclonal anti-Rabbit Cy3 conjugate (Jackson ImmunoResearch Labs, Cat#111-165-144, dil. 1:200), Goat polyclonal anti-Human Cy3 conjugate (dil. 1:200), Goat polyclonal anti-Hamster Cy5 conjugate (Jackson ImmunoResearch Labs, Cat# 127-175-160, dil. 1:200) were used for the staining.
Validation	The employed α-S.Tm LPS antibodies have been validated in references Moor et al. 2017, Nature and Sellin et al. 2014, Cell Host Microbe. The α-ICAM-1/CD54 antibody was used in reference Sellin et al. 2014, Cell Host Microbe to differentiate the intestinal epithelium from the lamina propria. WGA AF647 specificity was validated on Carnoy-fixed, paraffin embedded colon sections from untreated C57BL/6 mice. Goblet cells as well as the colonic mucus layer showed bright staining using this compound. The staining was comparable to adjacent tissue sections stained with α-Muc2 antibodies (Santa Cruz, Cat#sc-15334, dil. 1:250, not used in this study) and goat polyclonal anti-Rabbit Cy3 conjugate.

Animals and other organisms

Policy information about studies involving animals; ARRIVE guidelines recommended for reporting animal research

Laboratory animals	8-12 week old 129Sv/Ev mice from Jackson laboratories; Specified pathogen free status; Animals were bred in a SPF barrier facility and we used sex and age-matched experimental groups.
Wild animals	The study did not involve wild animals.
Field-collected samples	The study did not involve field-collected samples.